

Figure 1

Bcl-2	5	NREIVMKYIHYKLSQRGYEWDAAGDVGAAPPGAAPAPGIFSSQP	
Bcl-X _L	5	NRELVVDFLSYKLSQKGYSWSQFSDVEENRTEAPEG---TESE	
Bcl-2	88	VVHLTLRQAGDDFSRRYRRDFAEMSRQLHLTPFTARGRFATVV	130
Bcl-X _L	85	AVKQALREAGDEFELRYRRAFSDLTSQLHITPGTAYQSFEQVV	127
Bcl-2	131	EELFRDGVNWGRIVAFFEFGGVMCVESVNREMSPLVDNIALWM	173
Bcl-X _L	128	NELFRDGVNWGRIVAFFSFGGALCVESVDKEMQVLVSRIAAM	170
Bcl-2	174	TEYLNRLHTWIQDNGGWDAFVELYG	199
Bcl-X _L	171	ATYLNLDHLEPWIQENGGWDTFVELYG	196

Figure 2A

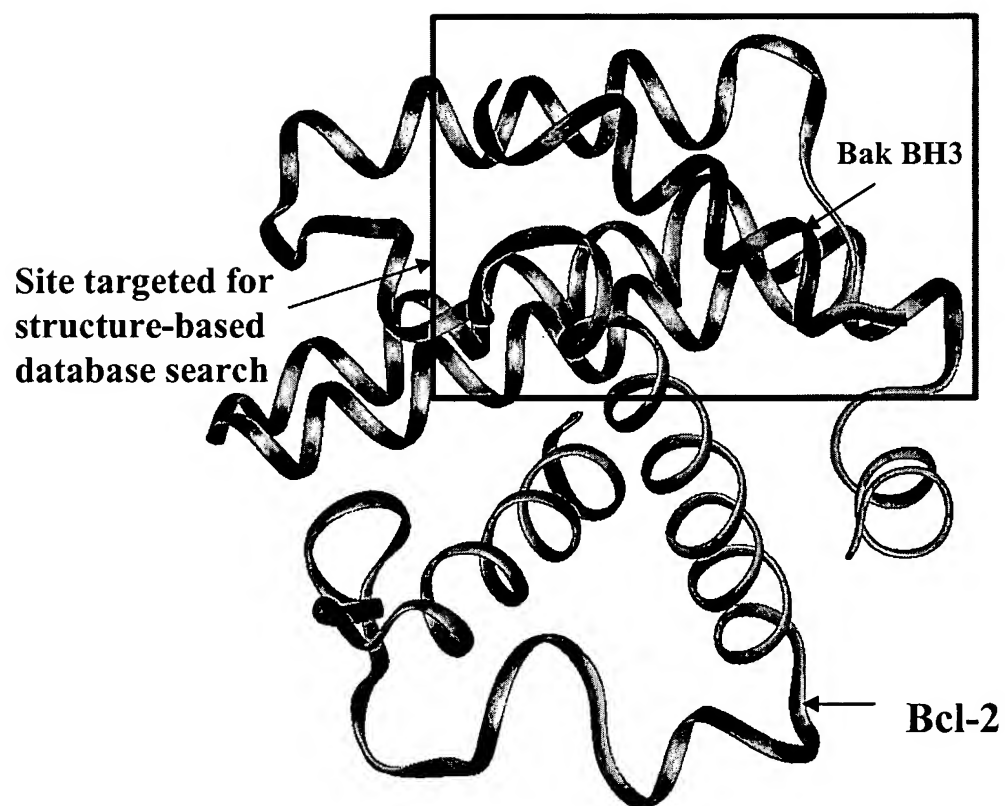


Figure 2B

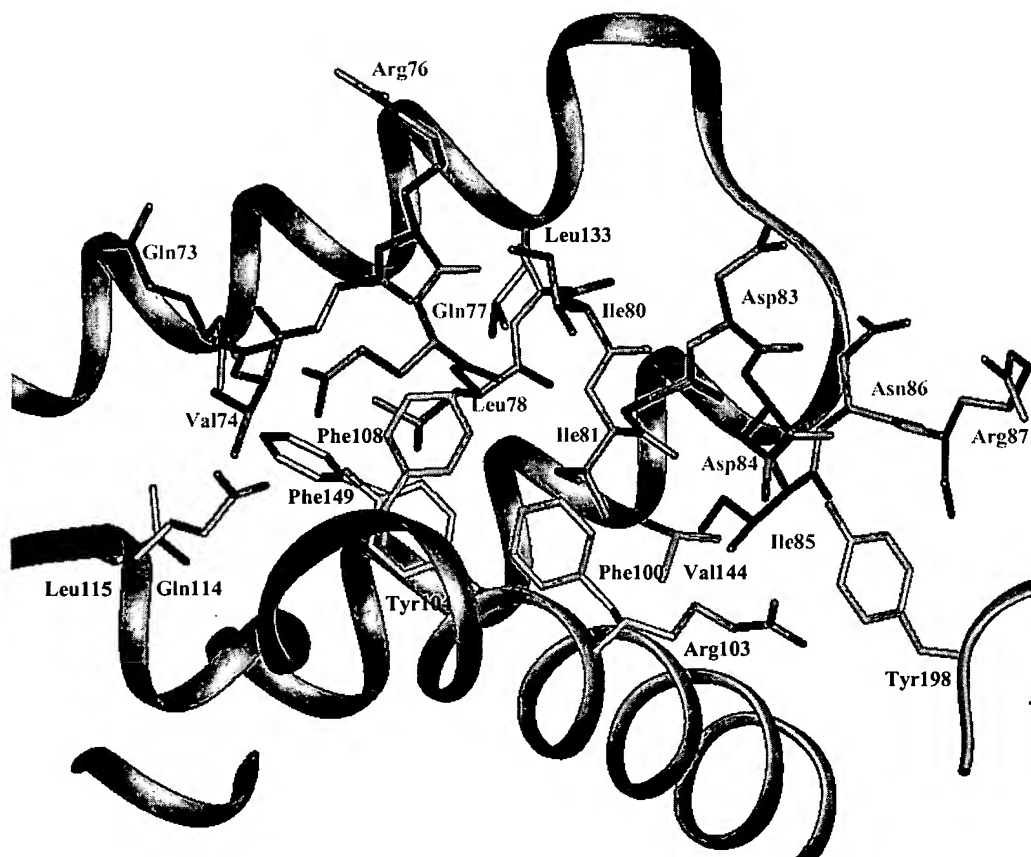


Figure 3

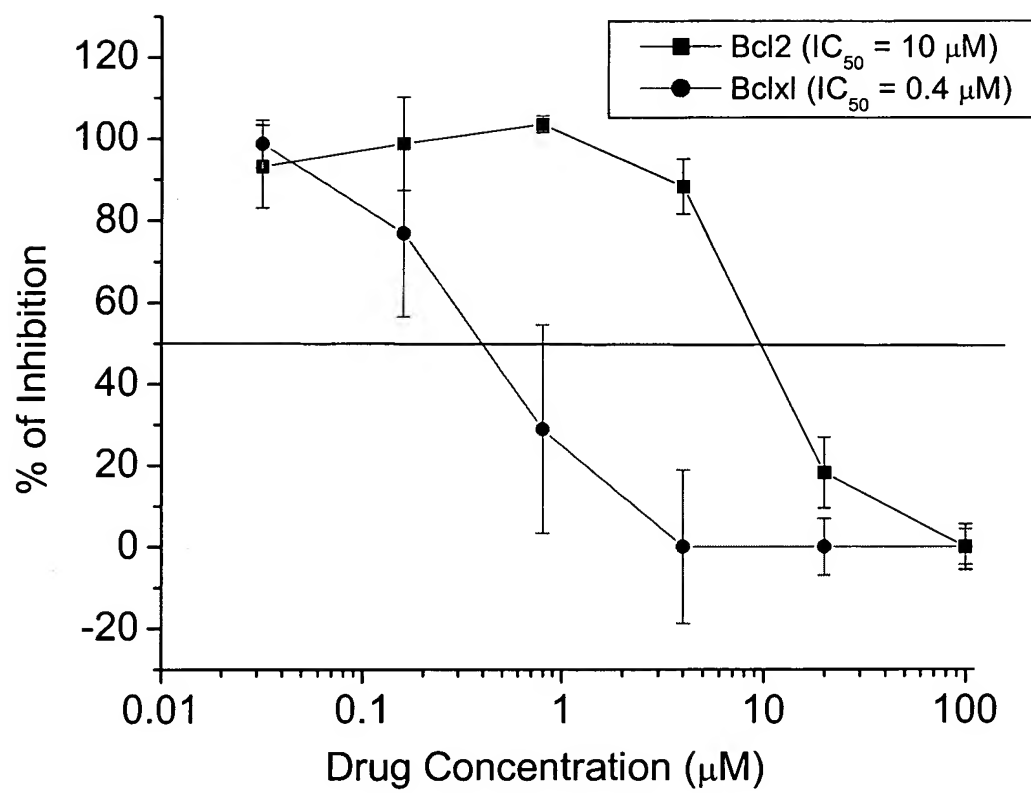


Figure 4

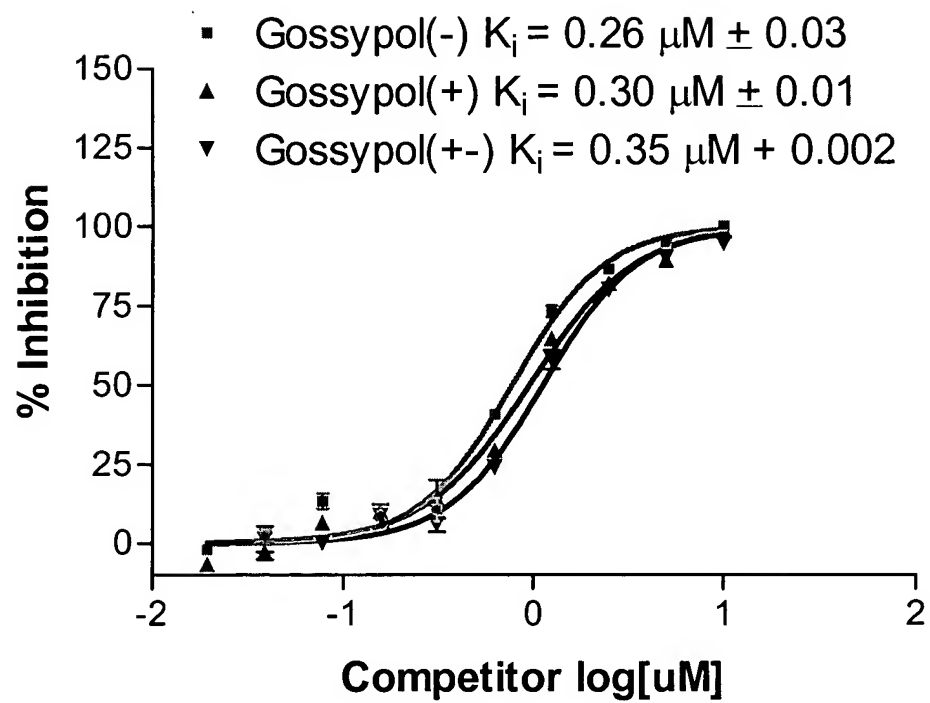


Figure 5

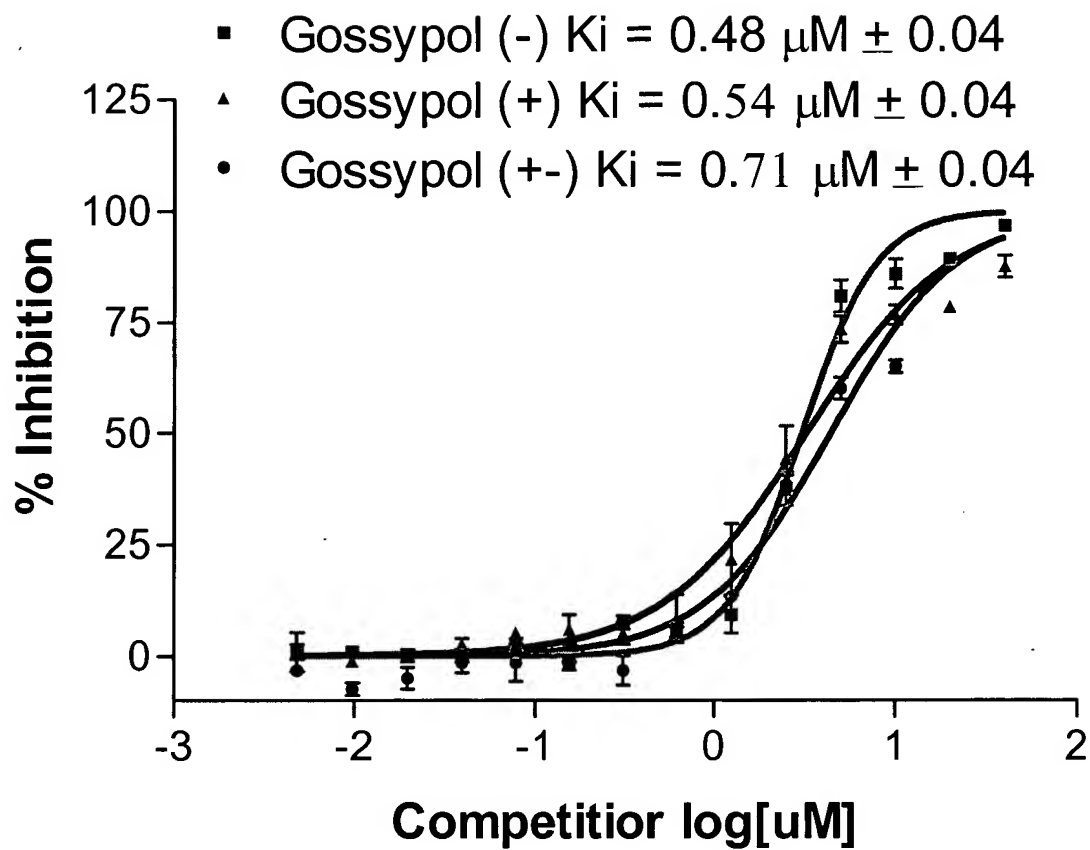


Figure 6A

Binding of gossypolone to Bcl-X_L

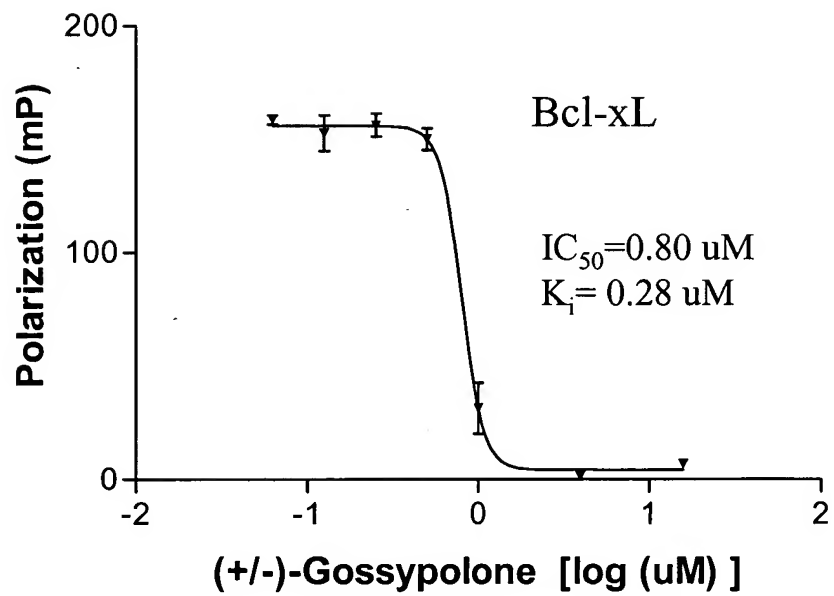


Figure 6B

Binding of Ethyl Schiff's base of (-)-Gossypol

IC₅₀ (after 18h30min) 7.346 uM
Ki 2.561 uM

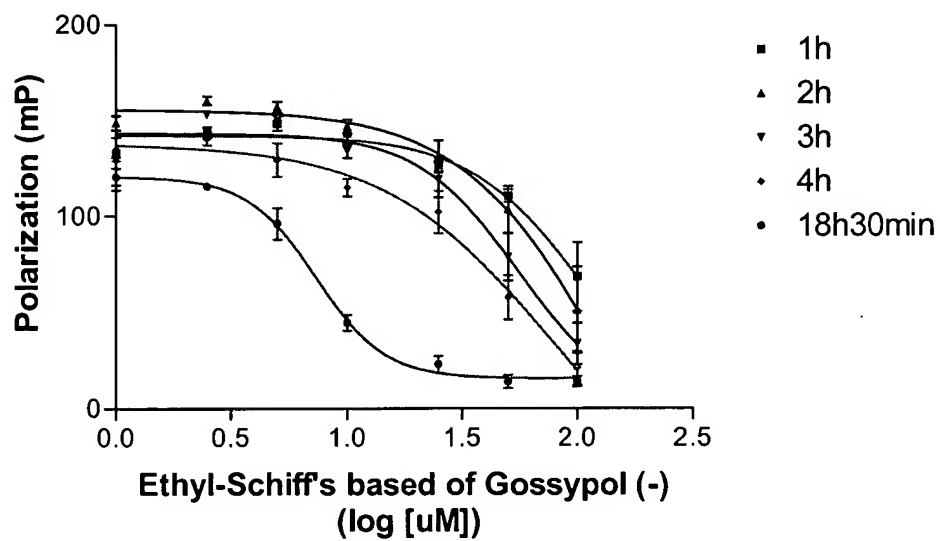
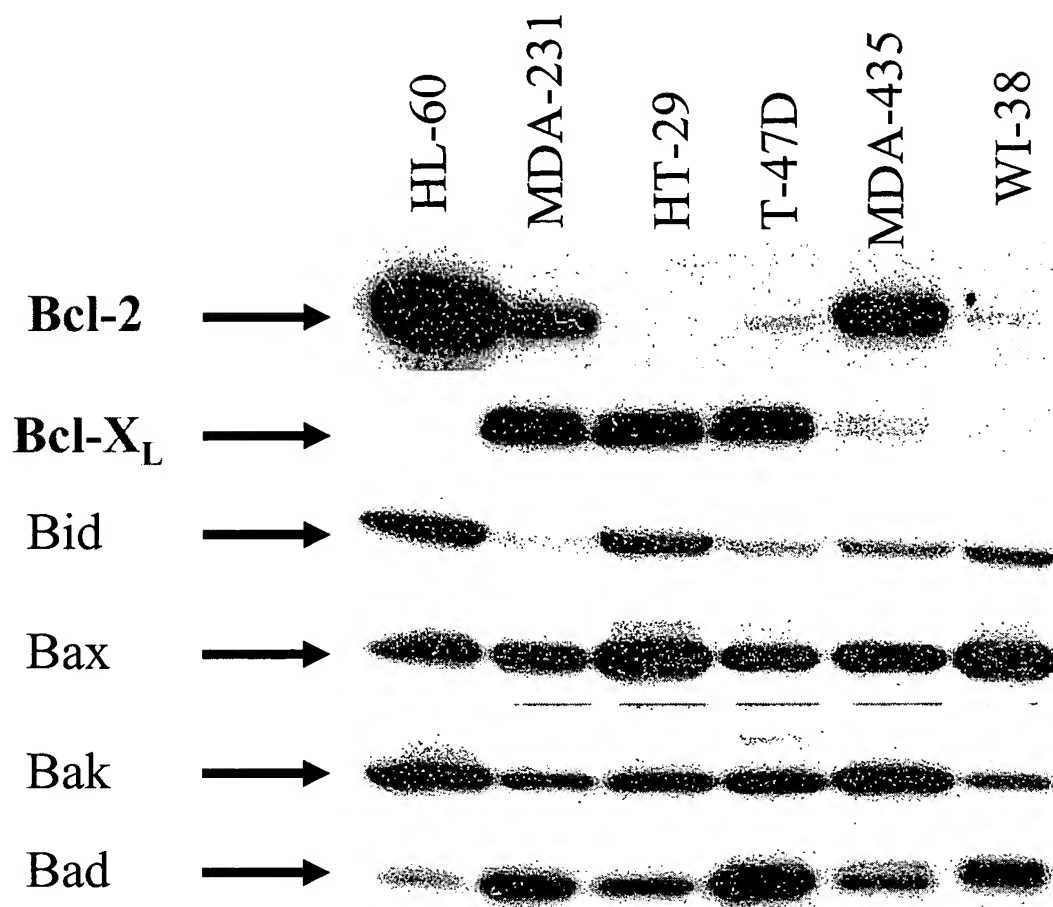
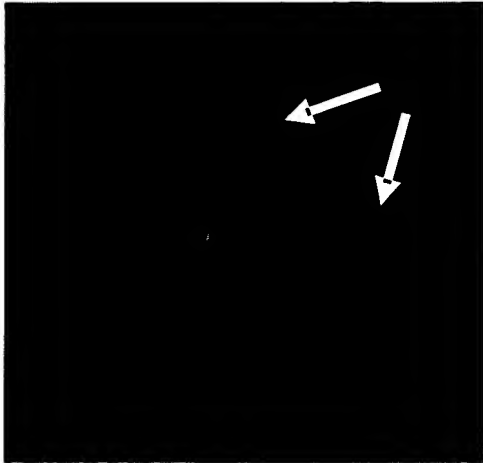


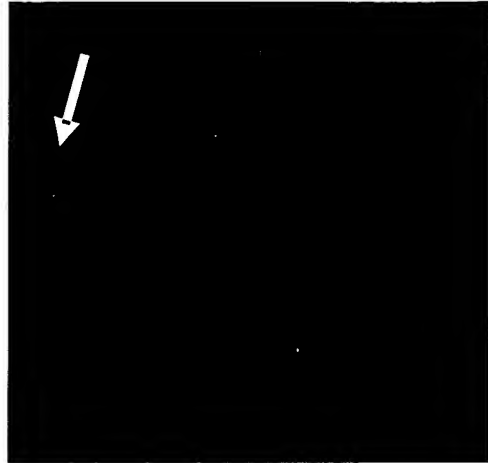
Figure 7





MDA-MB-231

Figure 8A



WI-38

Figure 8B

BEST AVAILABLE COPY

Figure 9

MDA-MB-231

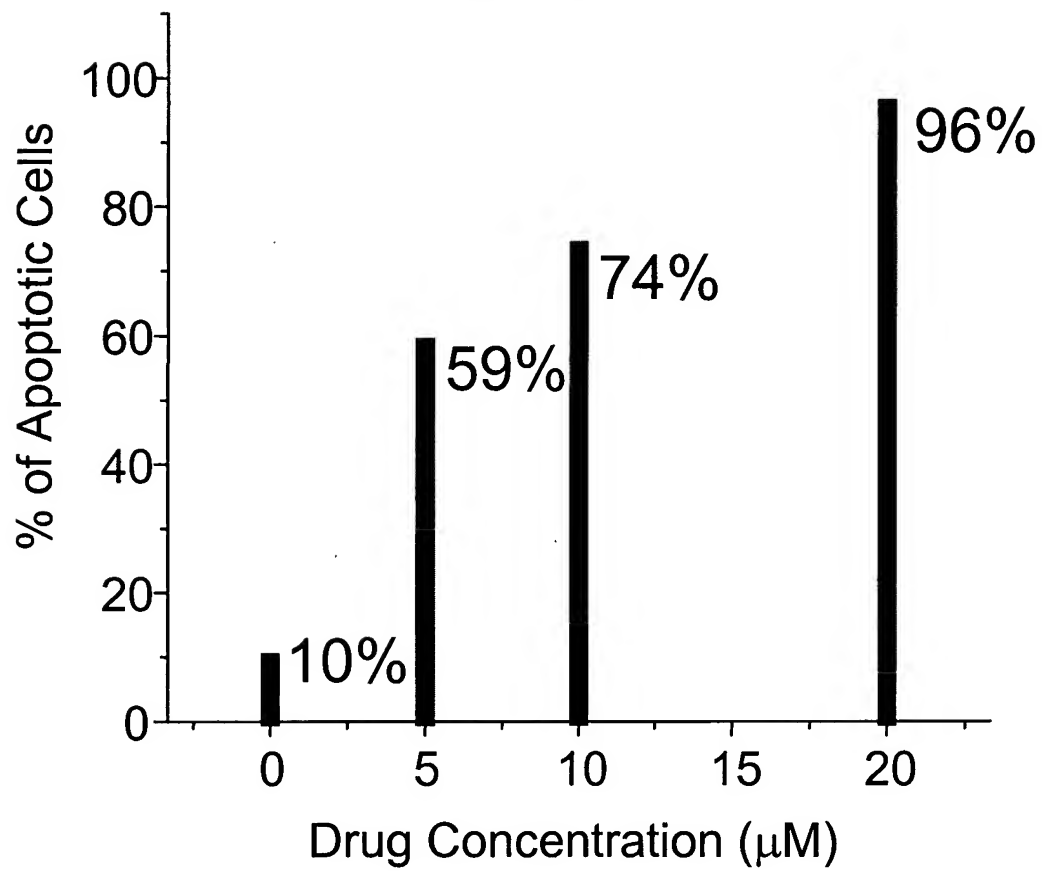


Figure 10

T-47D

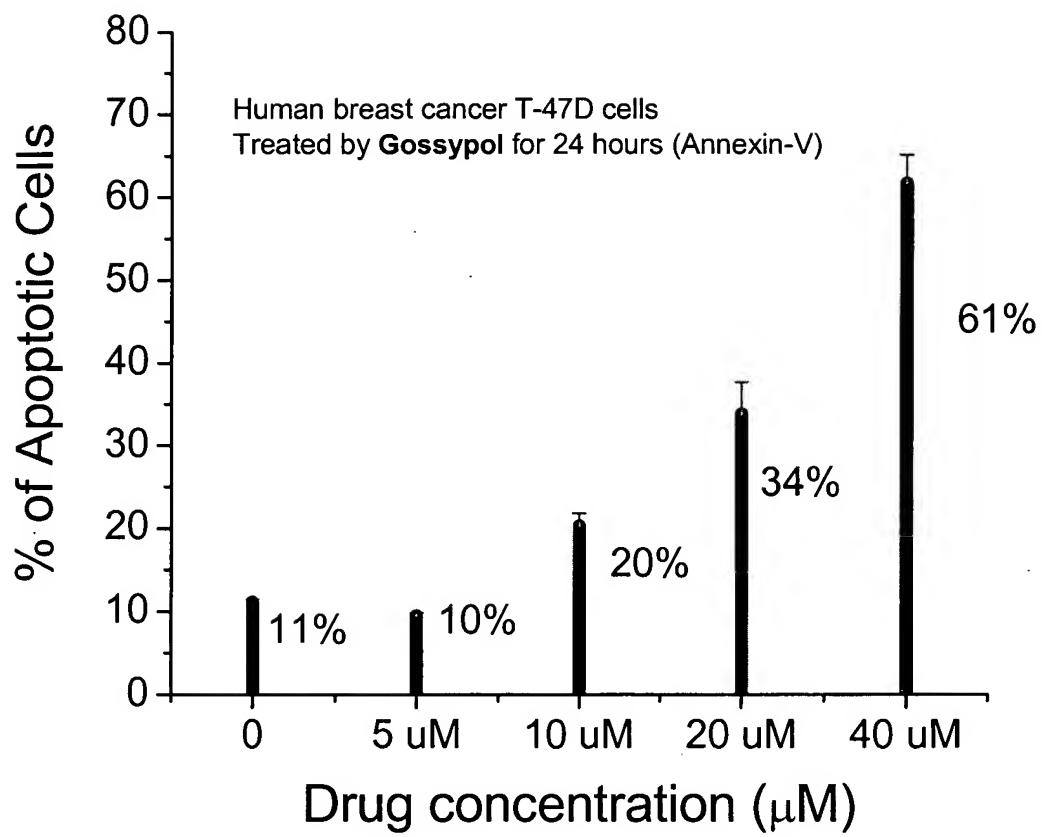
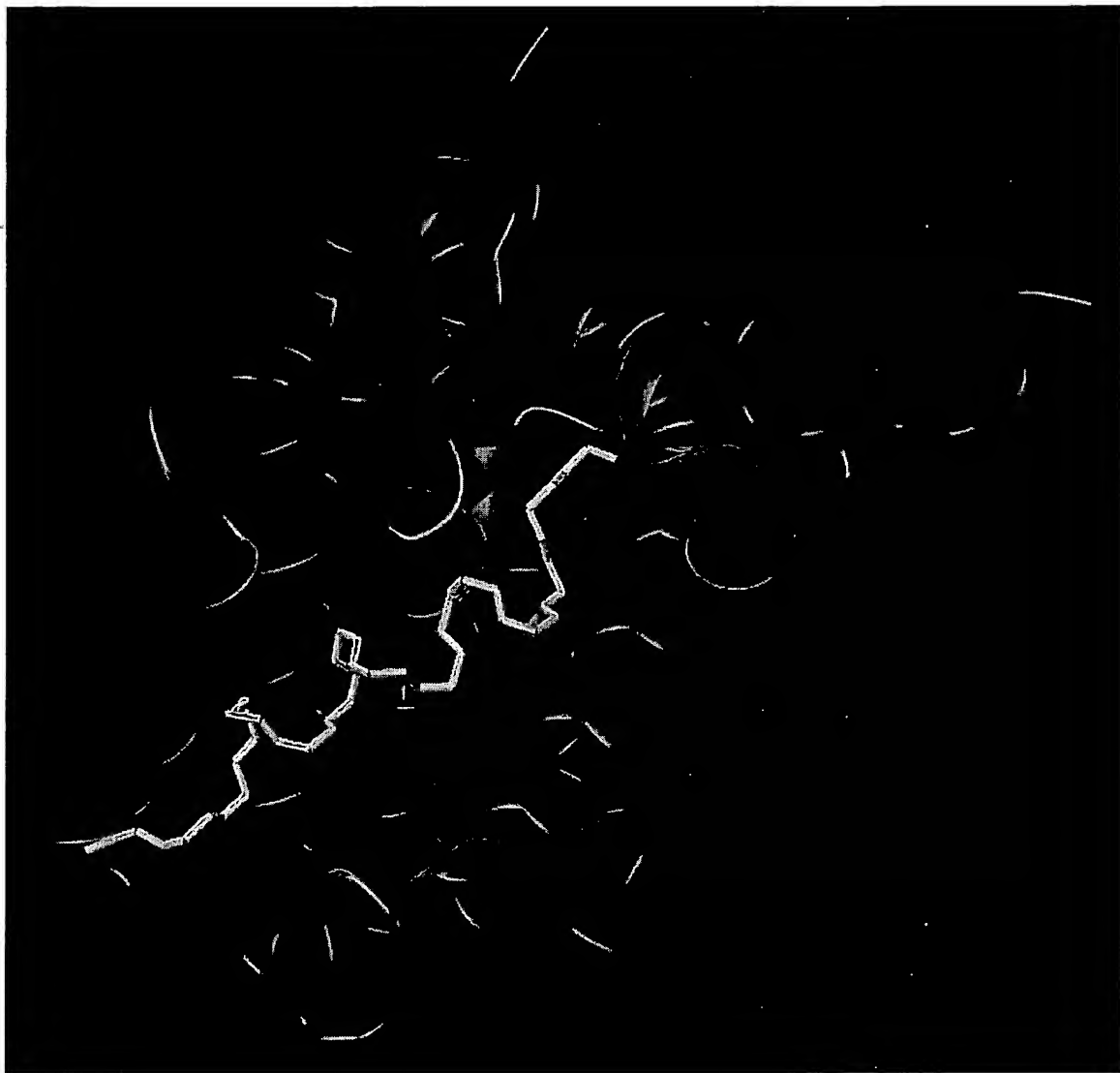


Figure 11A



BEST AVAILABLE COPY

Figure 11B

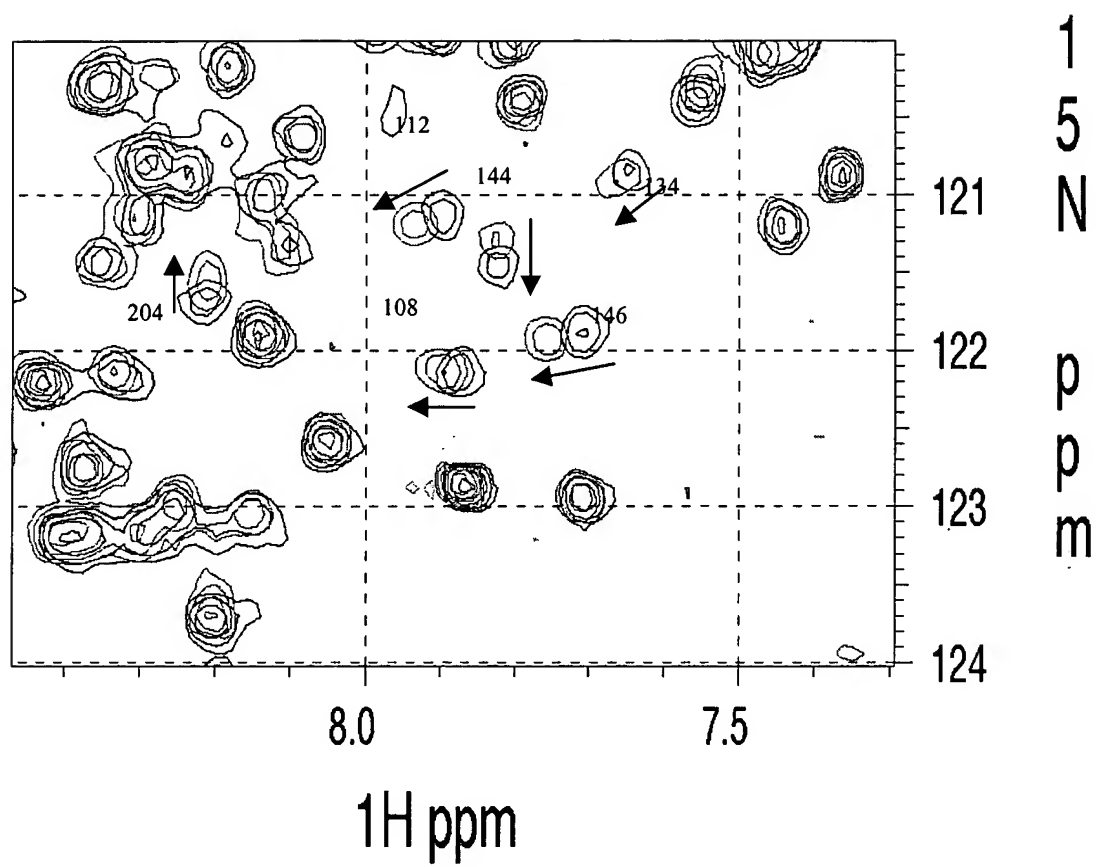


Figure 11C

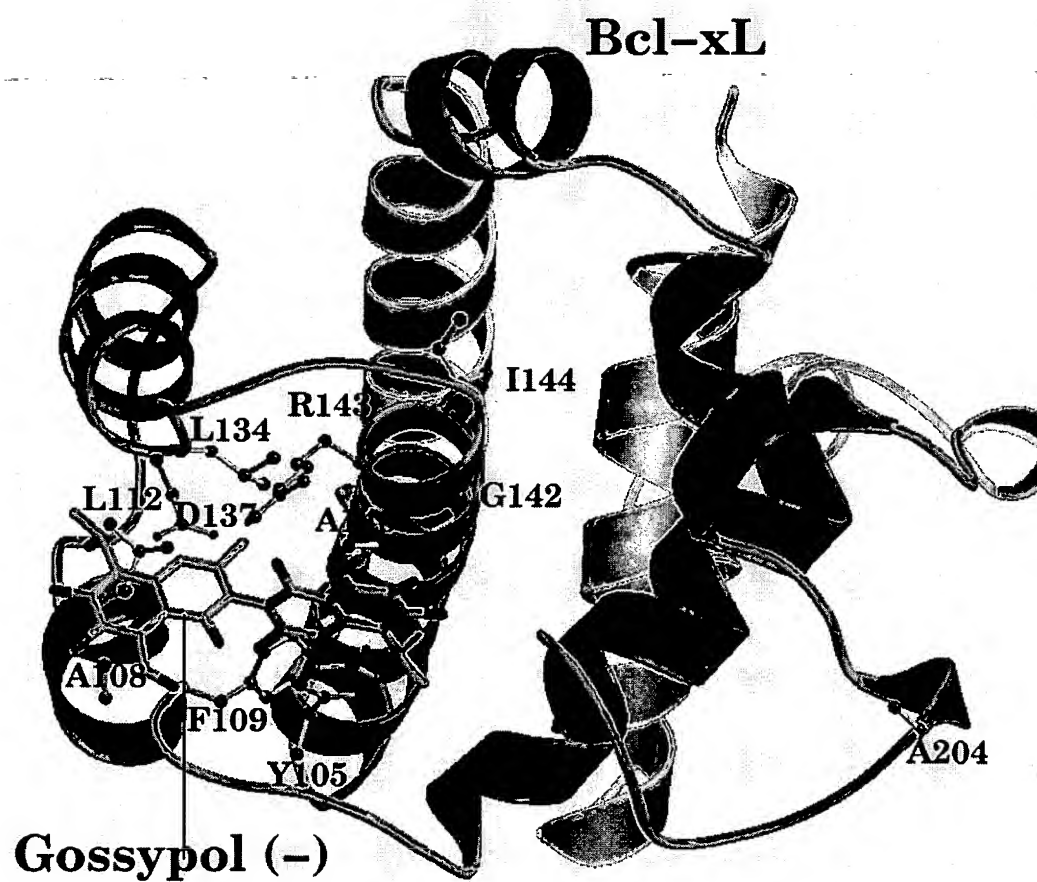


Figure 12

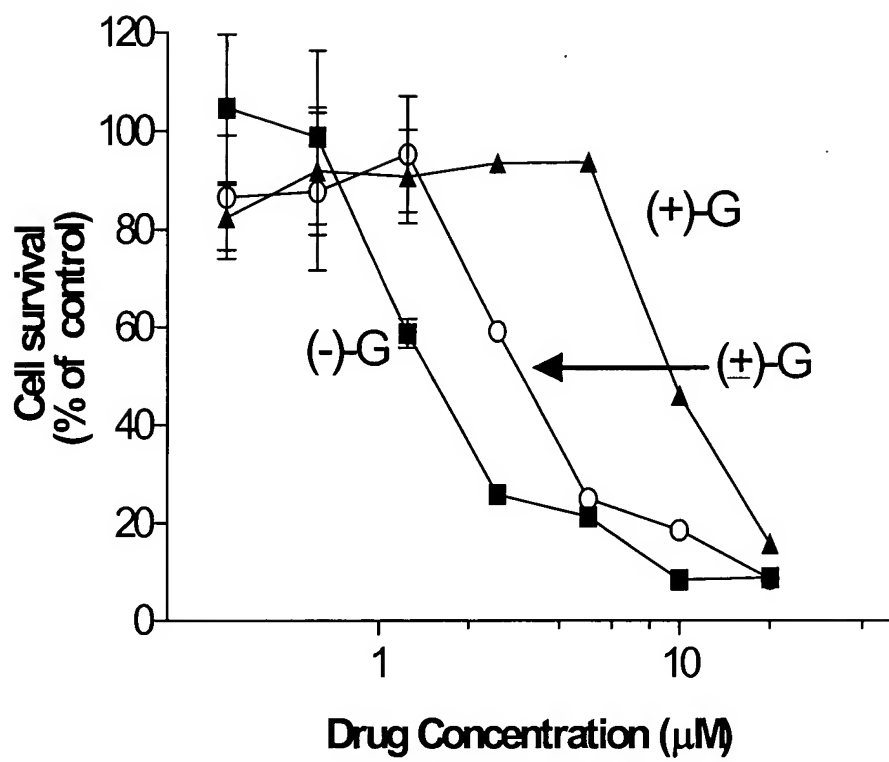


Figure 13



Figure 14

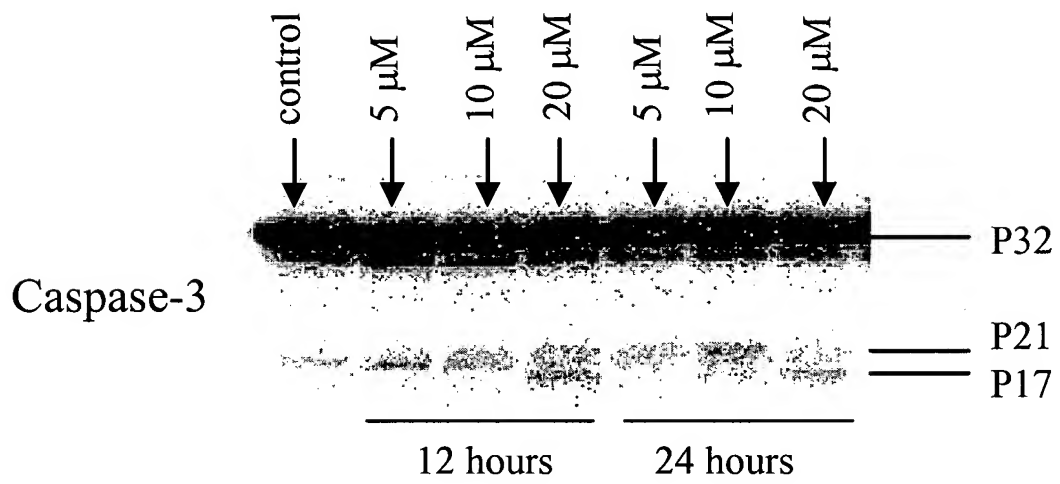


Figure 15

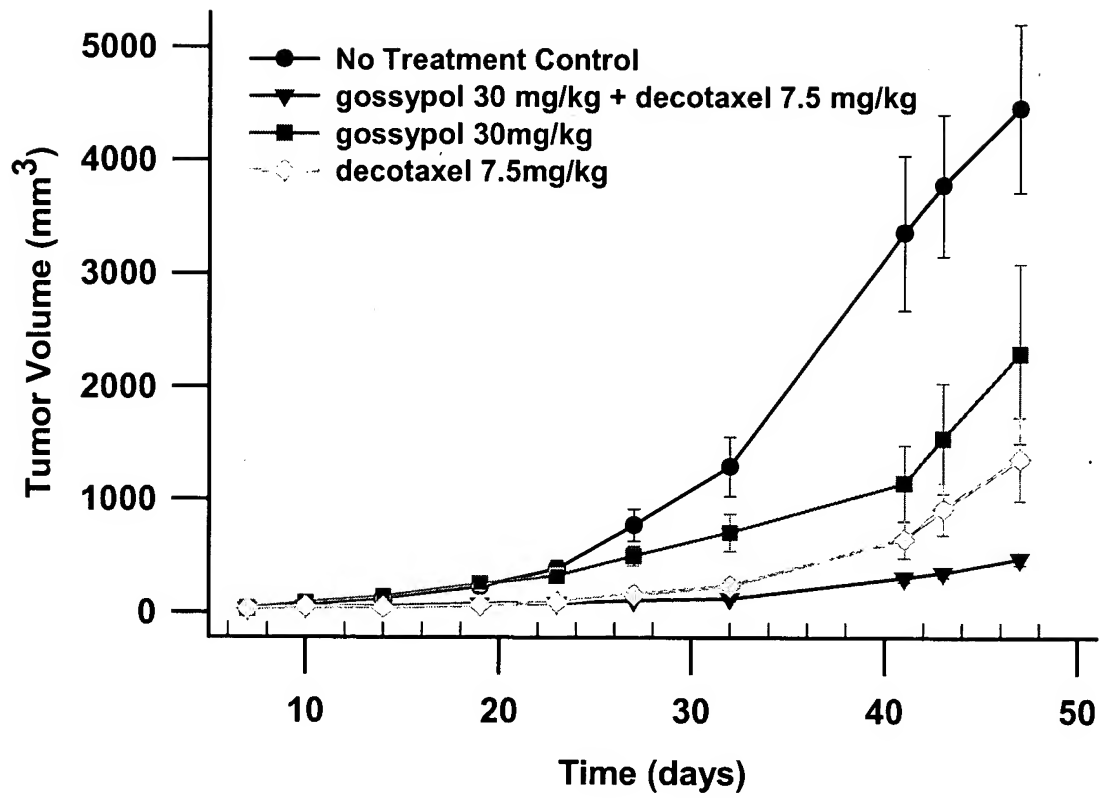
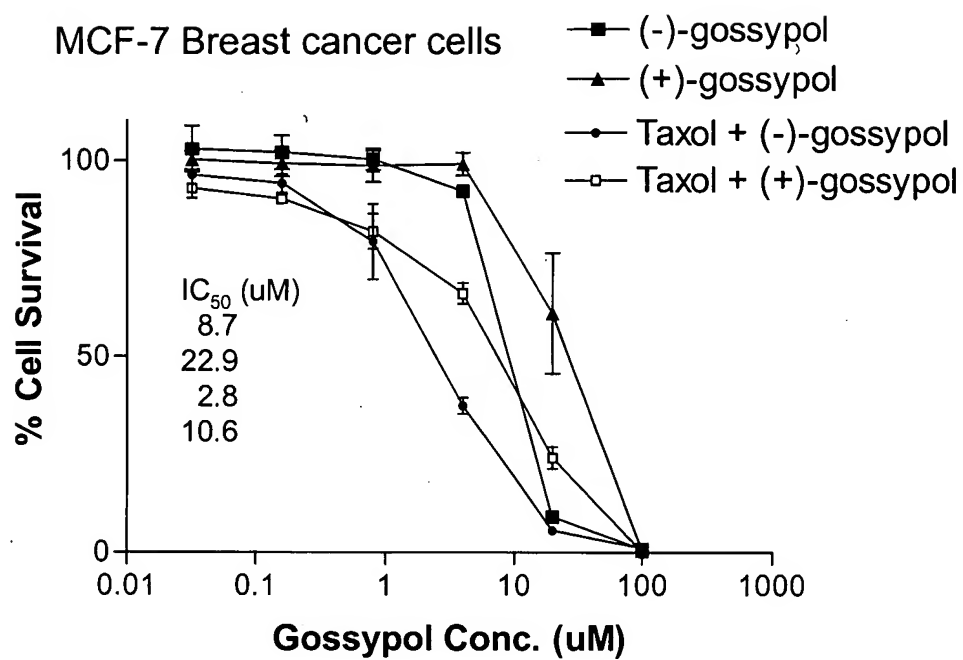


Figure 16



This experiment used 100:1 ratio between (-)-gossypol and Taxol, and between (+)-gossypol and Taxol

Figure 17A

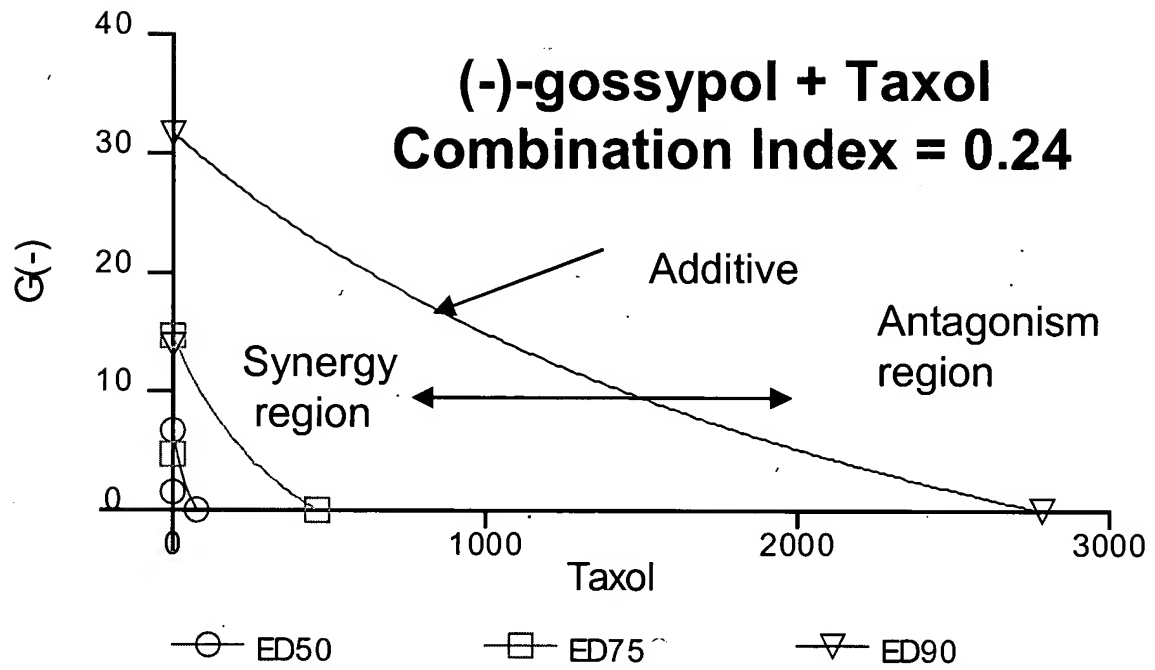


Figure 17B

MDA-MB-231 DOX + G- 1:2.5uM

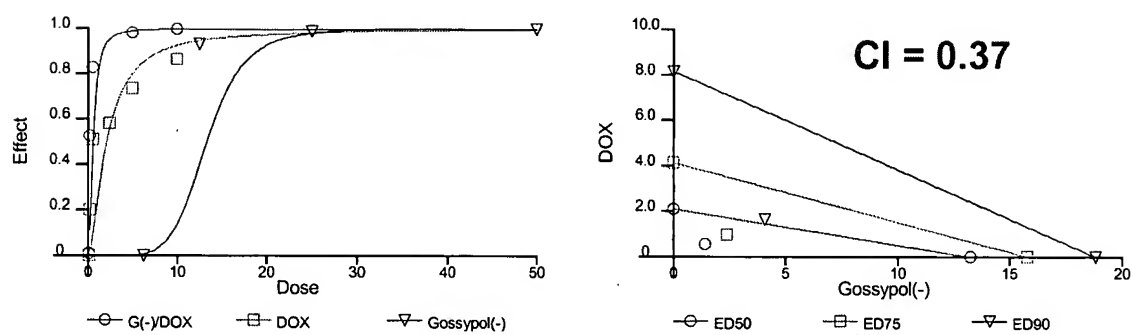


Figure 18

Effect of (-)-gossypol on inhibition of tumor growth of human breast cancer xenograft MDA-231

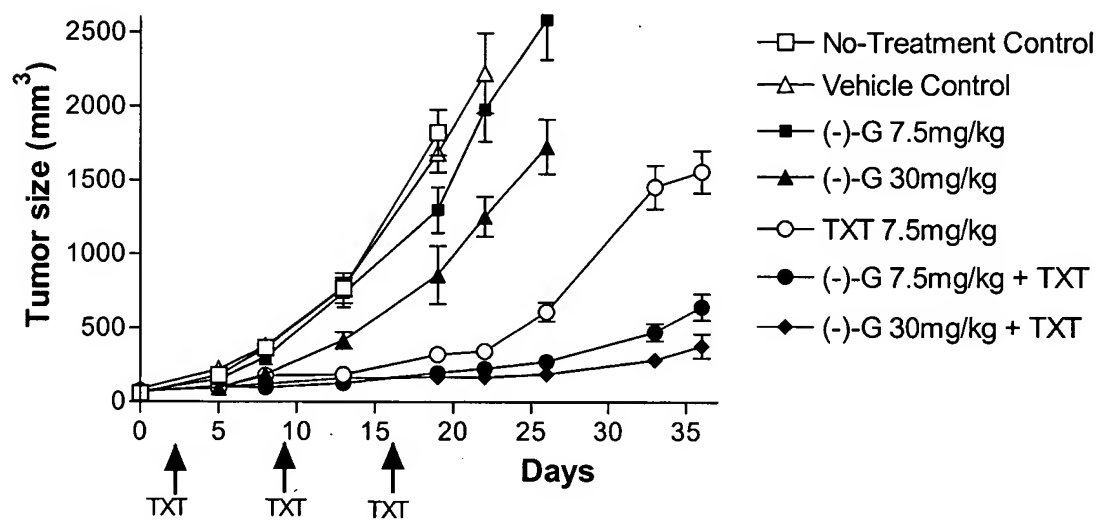


Figure 19

Effect of (-)-gossypol on inhibition of tumor growth of human breast cancer xenograft MDA-231

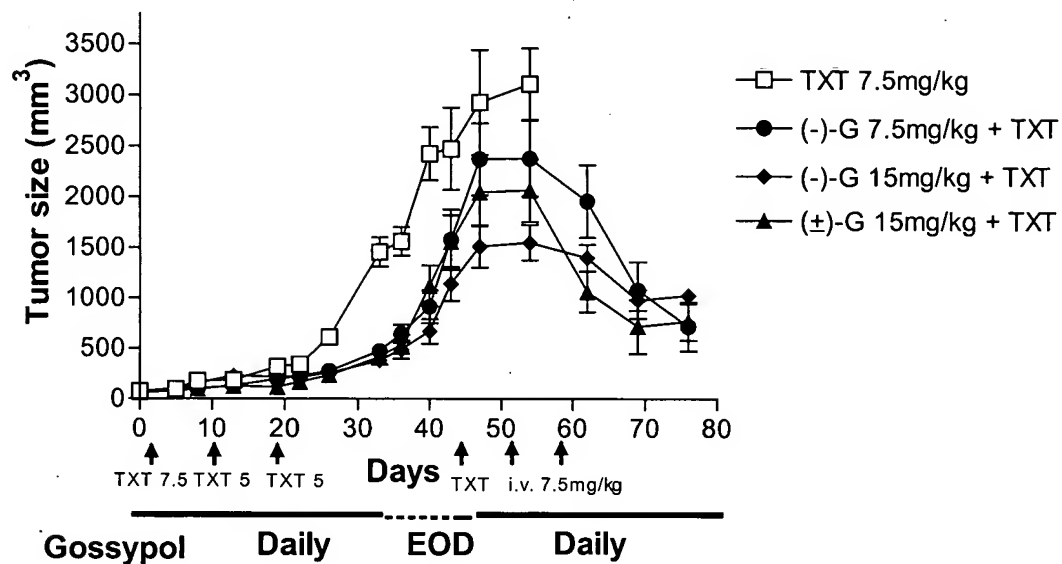


Figure 20

Effect of (-)-gossypol on inhibition of tumor growth of human non-small cell lung carcinoma cell xenograft A-549

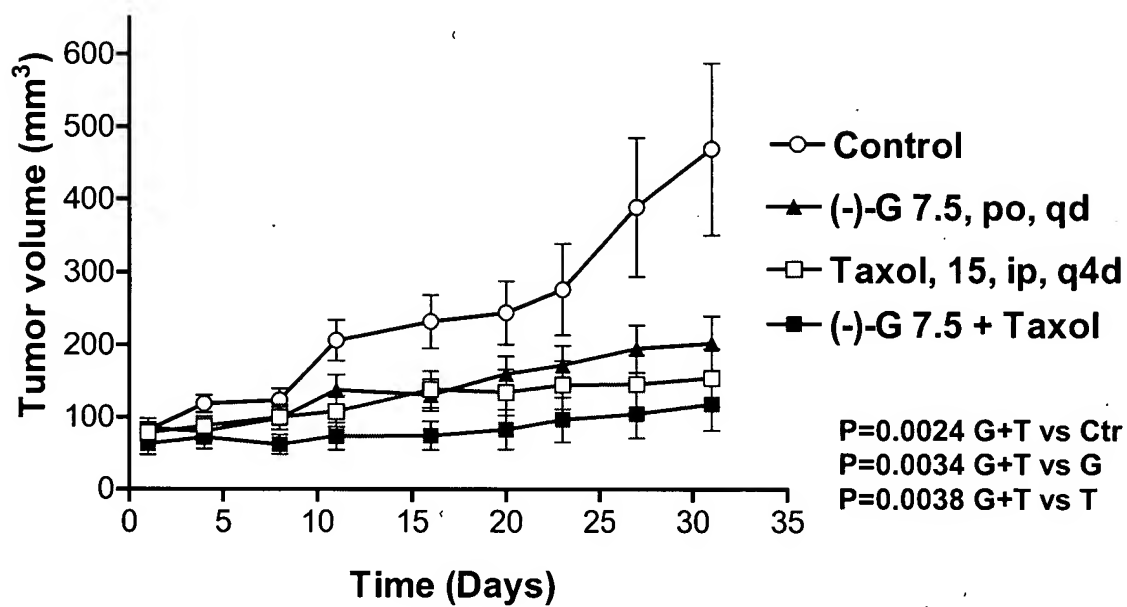


Figure 21

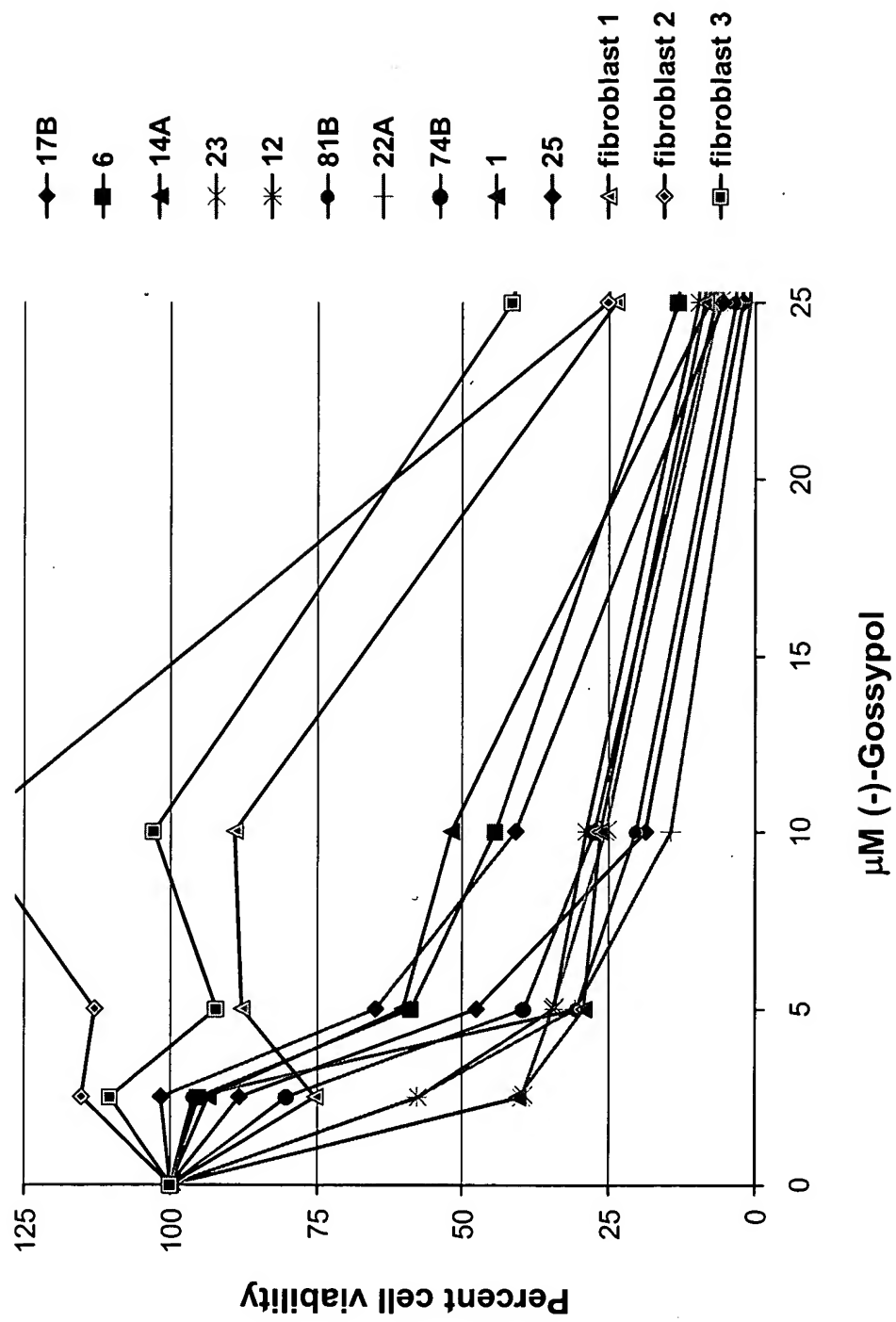


Figure 22

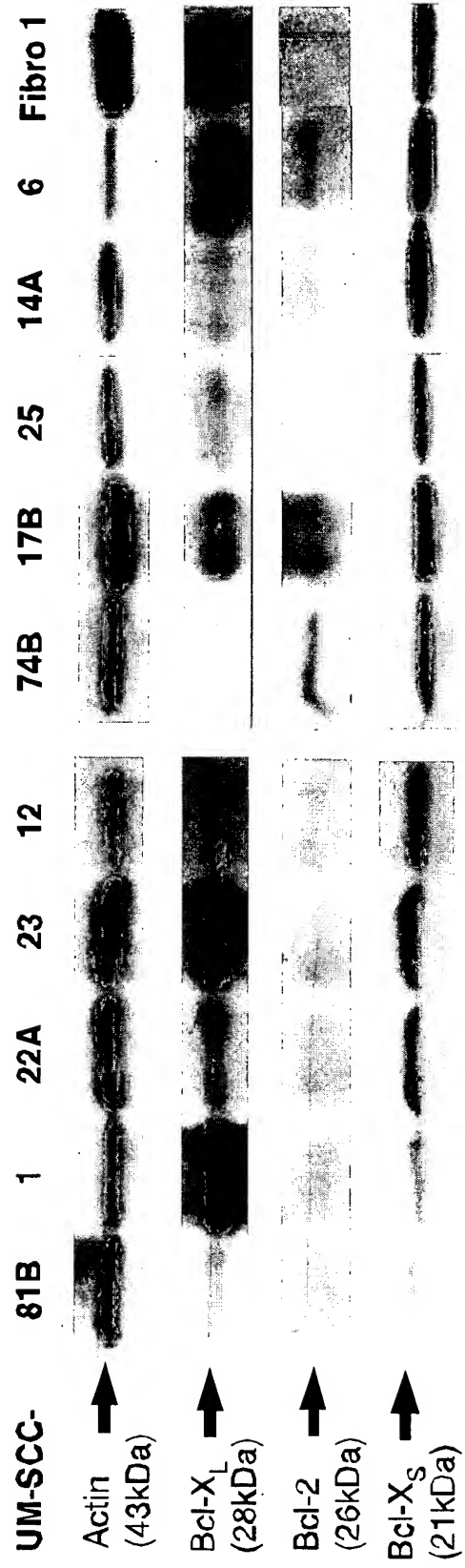
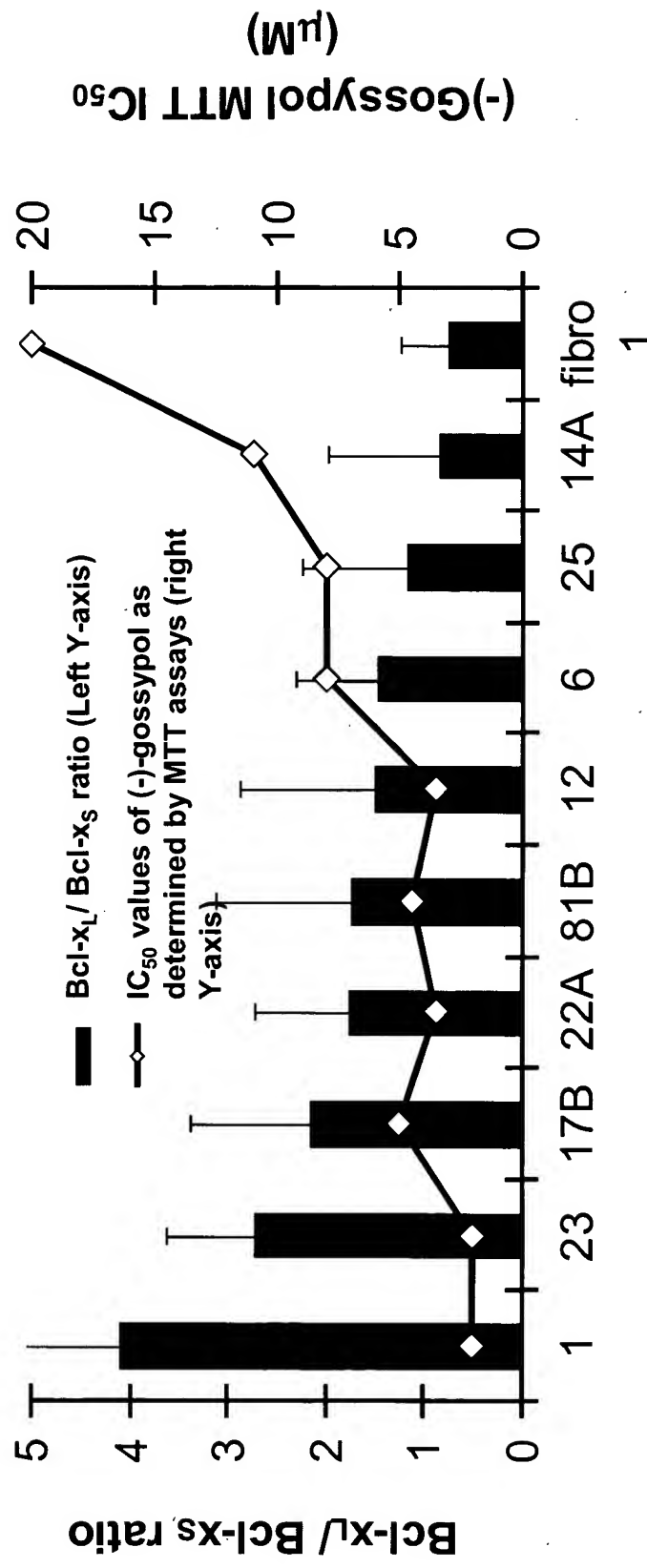


Figure 23



UM-SCC cell line

Figure 24A

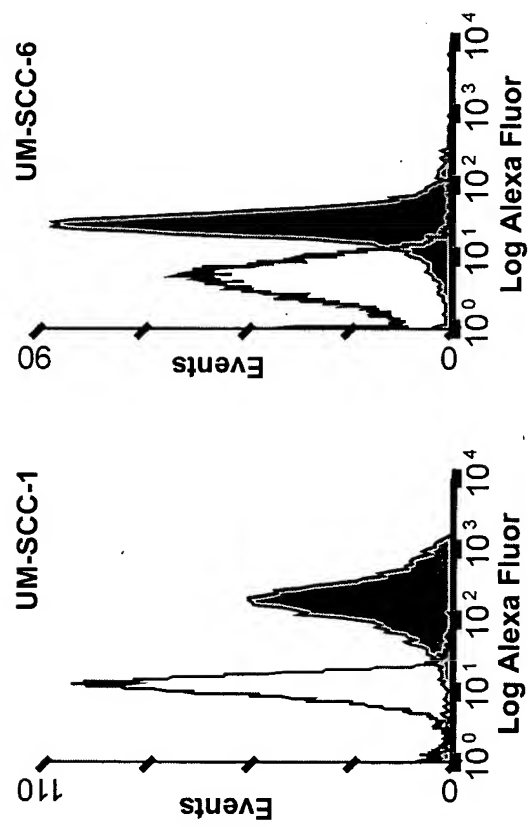


Figure 24B

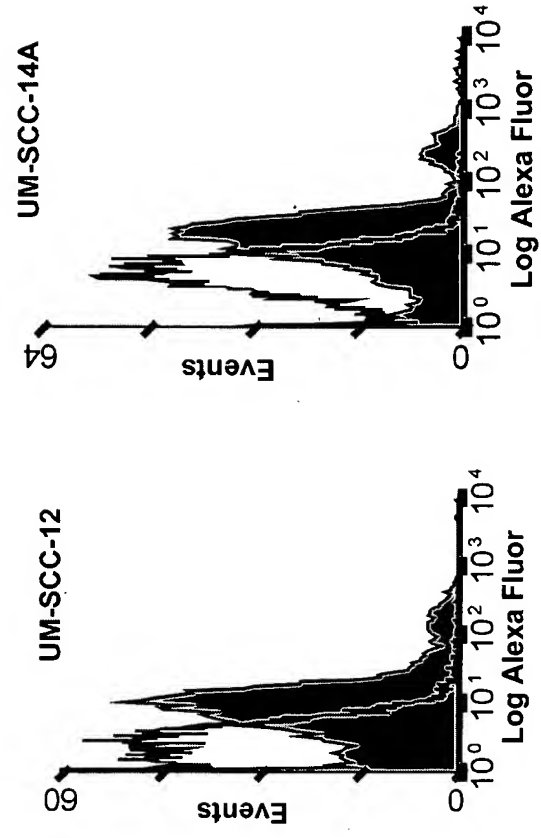


Figure 24C

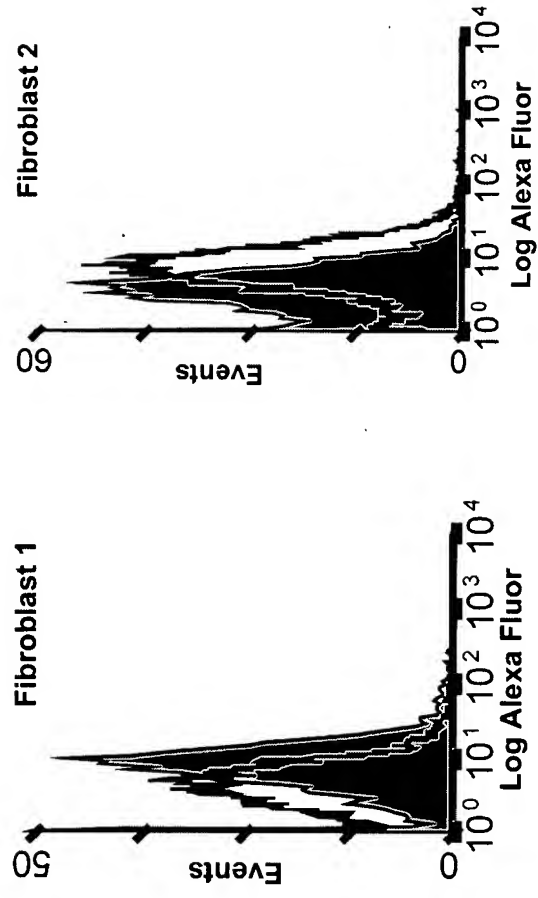
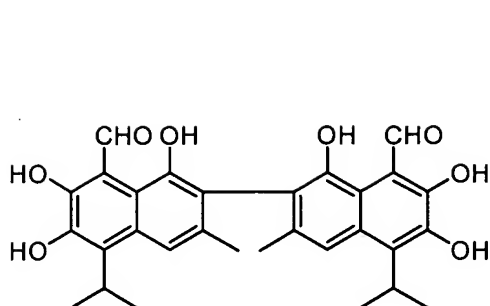
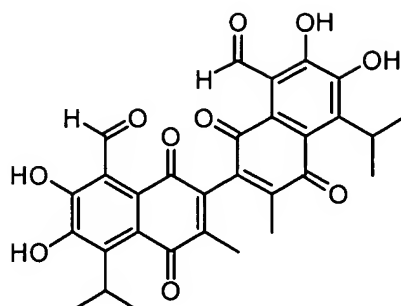


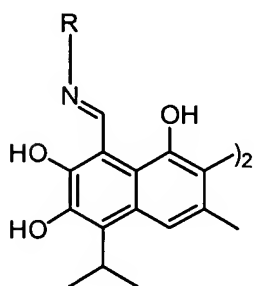
Figure 25



Gossypol

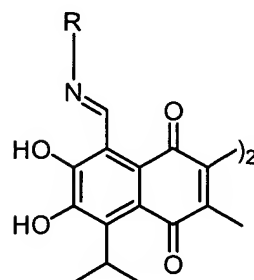


Gossypolone



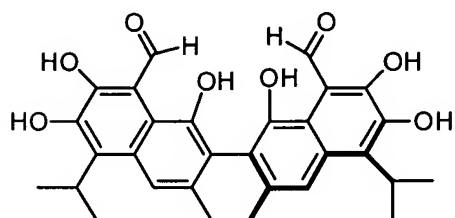
R = aliphatic or aromatic group

Schiff's base of Gossypol

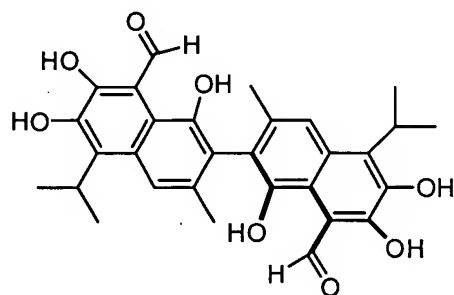


R = aliphatic or aromatic group

Schiff's base of Gossypolone



(-)-(R)-Gossypol



(+)-(S)-Gossypol

Figure 26

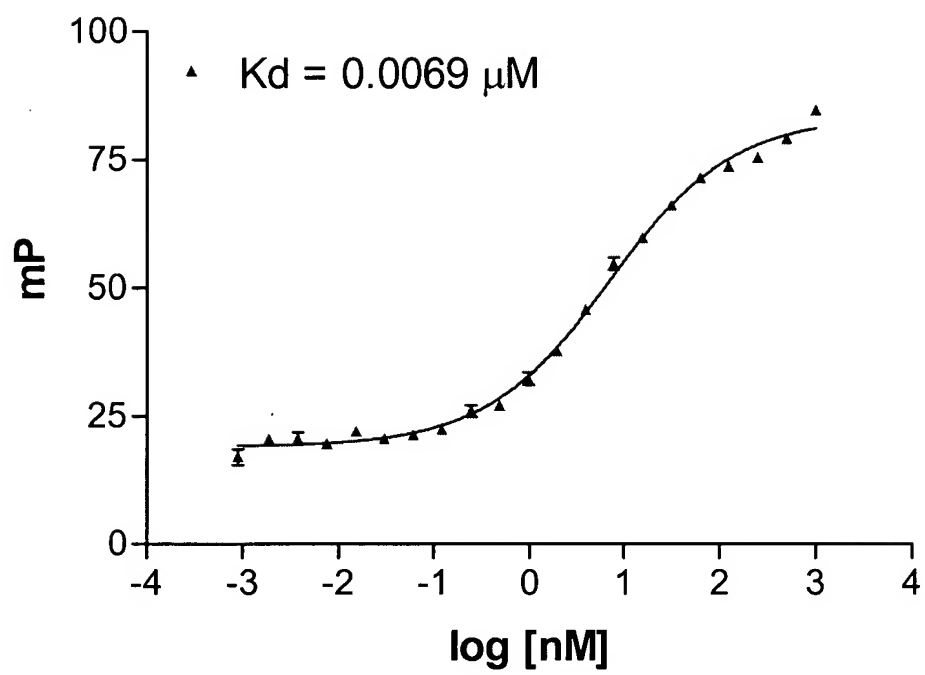


Figure 27

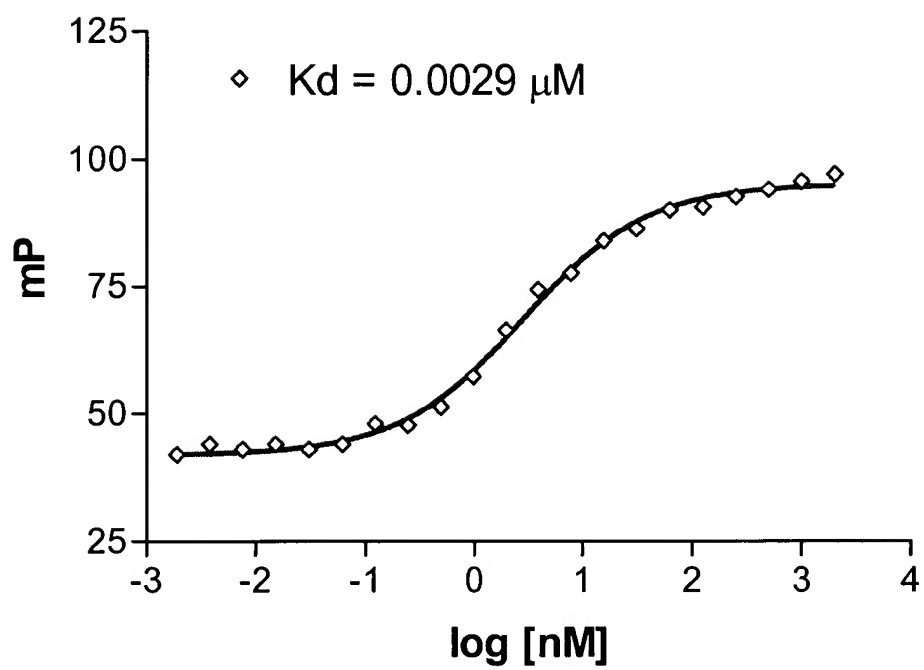


Figure 28A

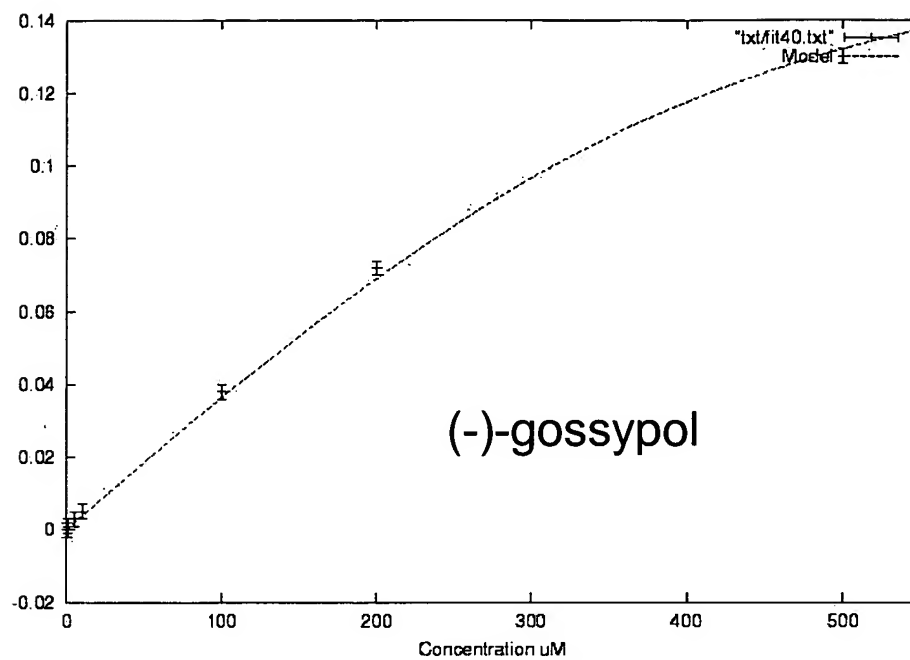


Figure 28B

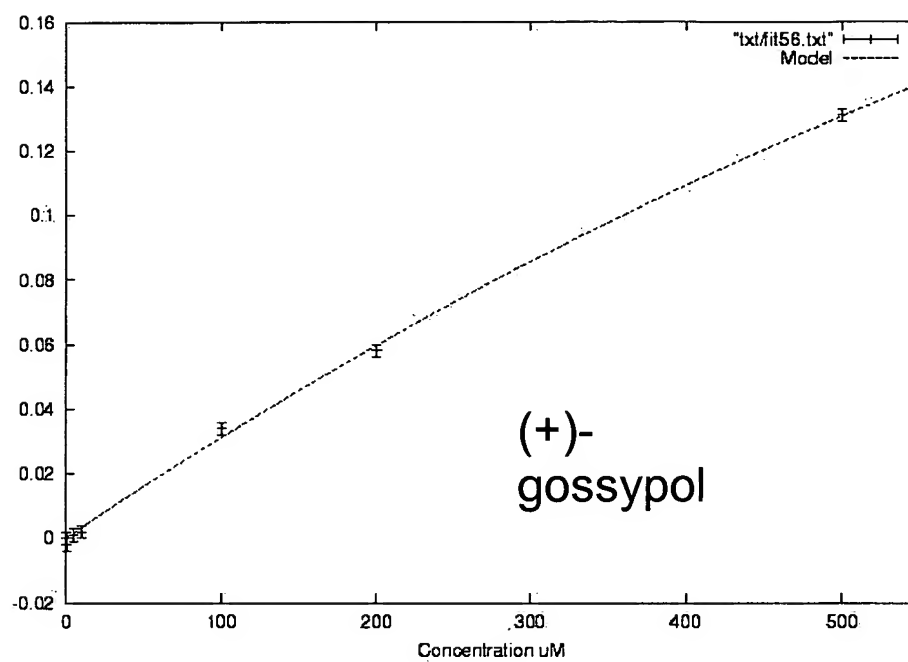


Figure 29

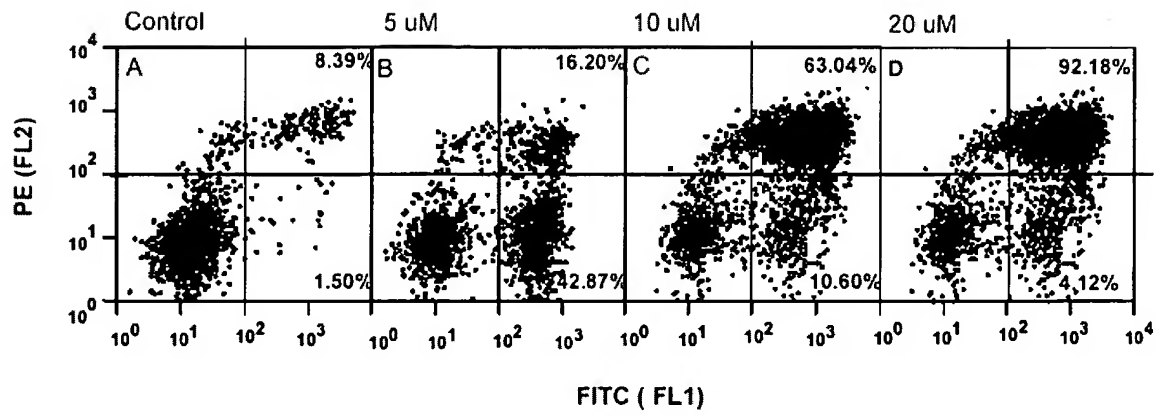


Figure 30

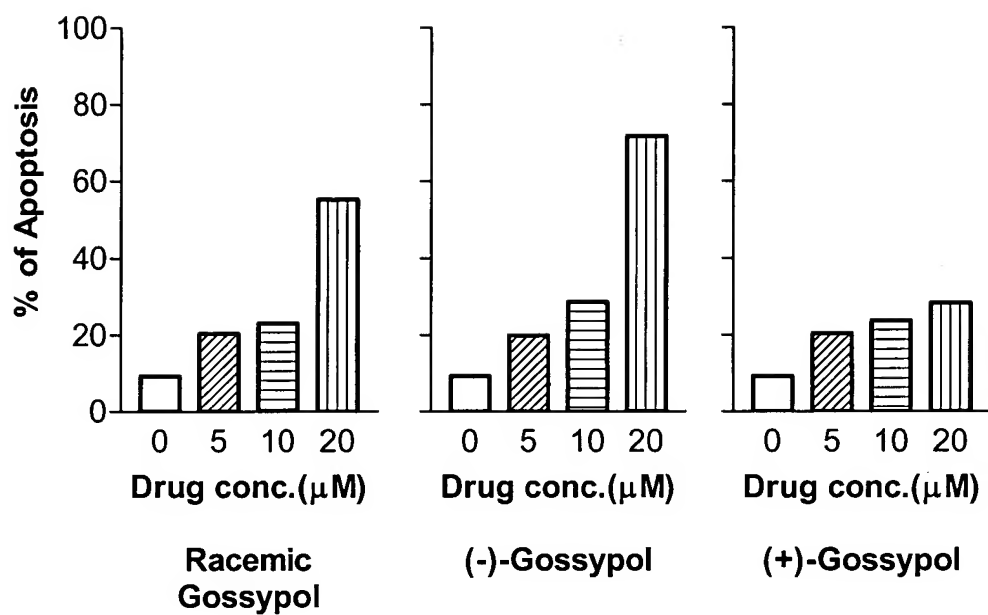


Figure 31

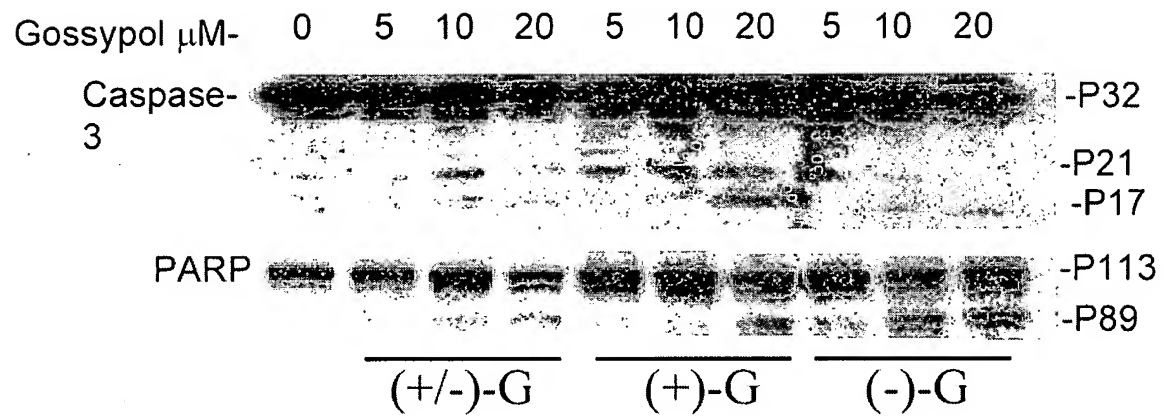


Figure 32A

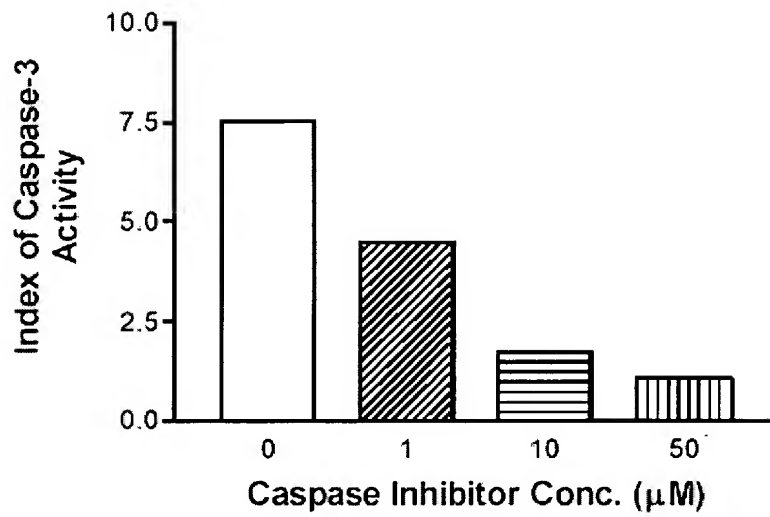


Figure 32B

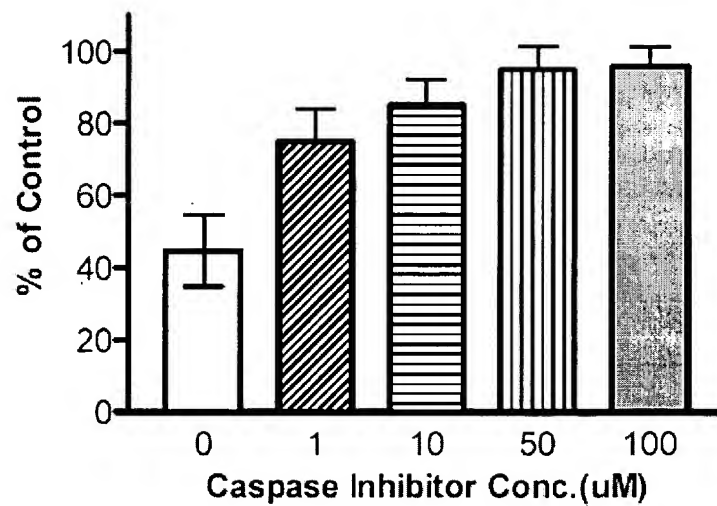


Figure 33

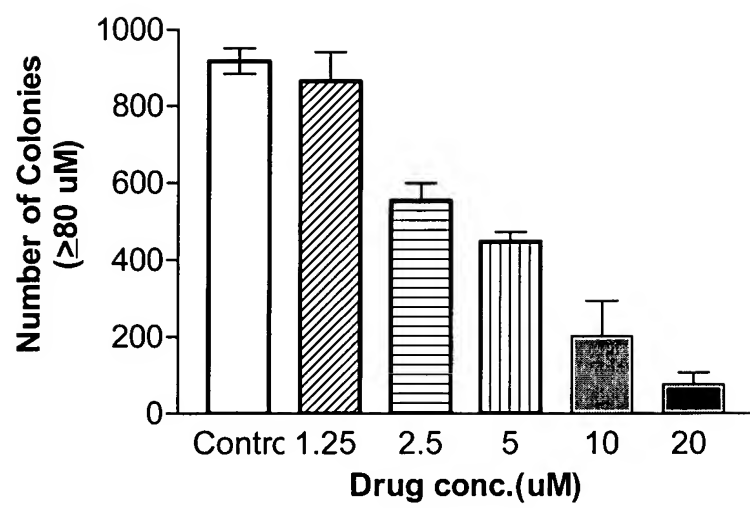


Figure 34

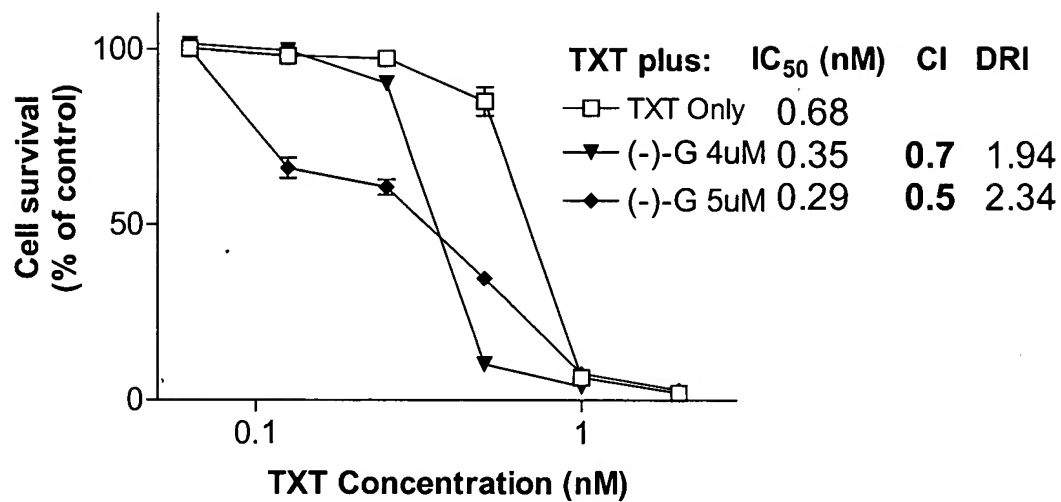


Figure 35A

In vitro effects of gossypol(-) in combination with various doses of radiation on PC-3 clonogenic assays

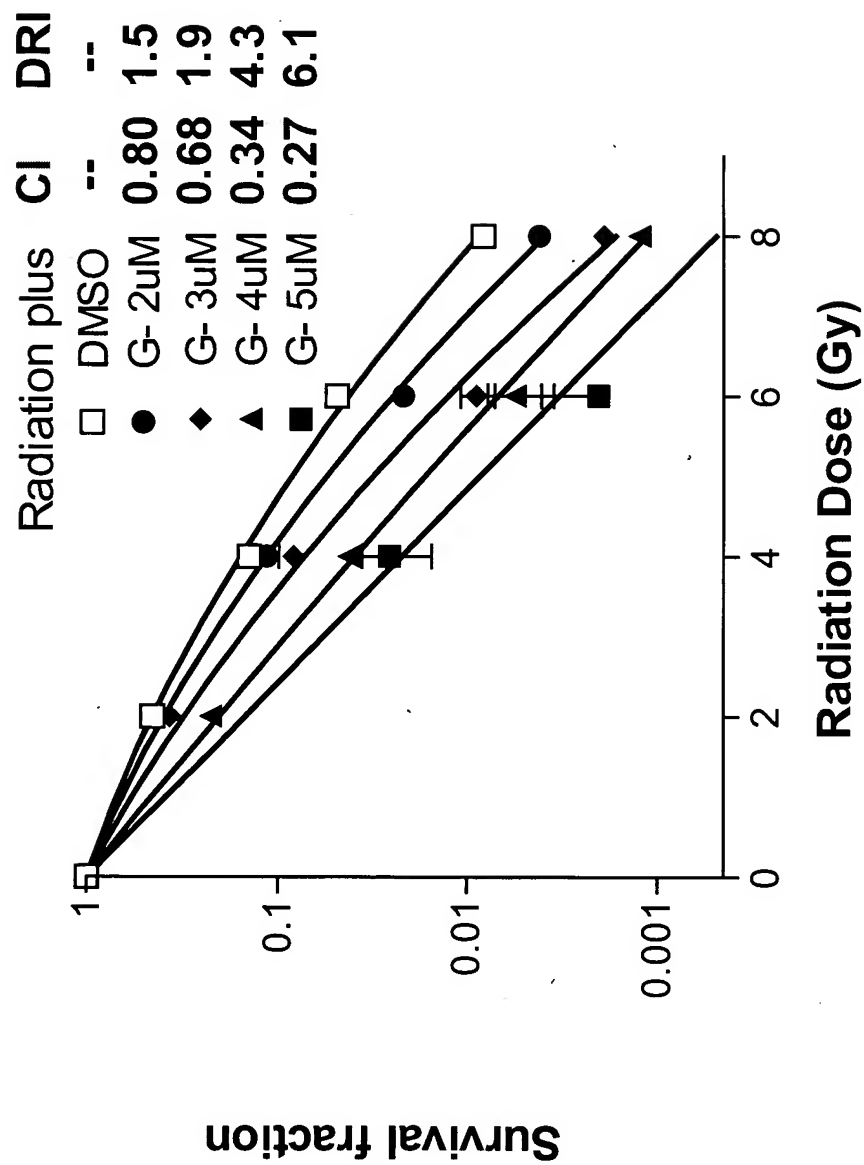


Figure 35B

G- μ M	0	1	2	3	4	5
D bar = Mean inactivation dose	2.22	2.06	1.95	1.63	1.26	1.05
Gy(1%)= Dose required for 1% cell survival	7.84	7.11	7.03	6.25	5.59	4.84
SF(2Gy)= Survival fraction at 2Gy	0.45	0.43	0.4	0.31	0.21	0.15

Figure 36

(-)-gossypol in combination with radiation in an androgen-independent prostate PC-3 xenograft model

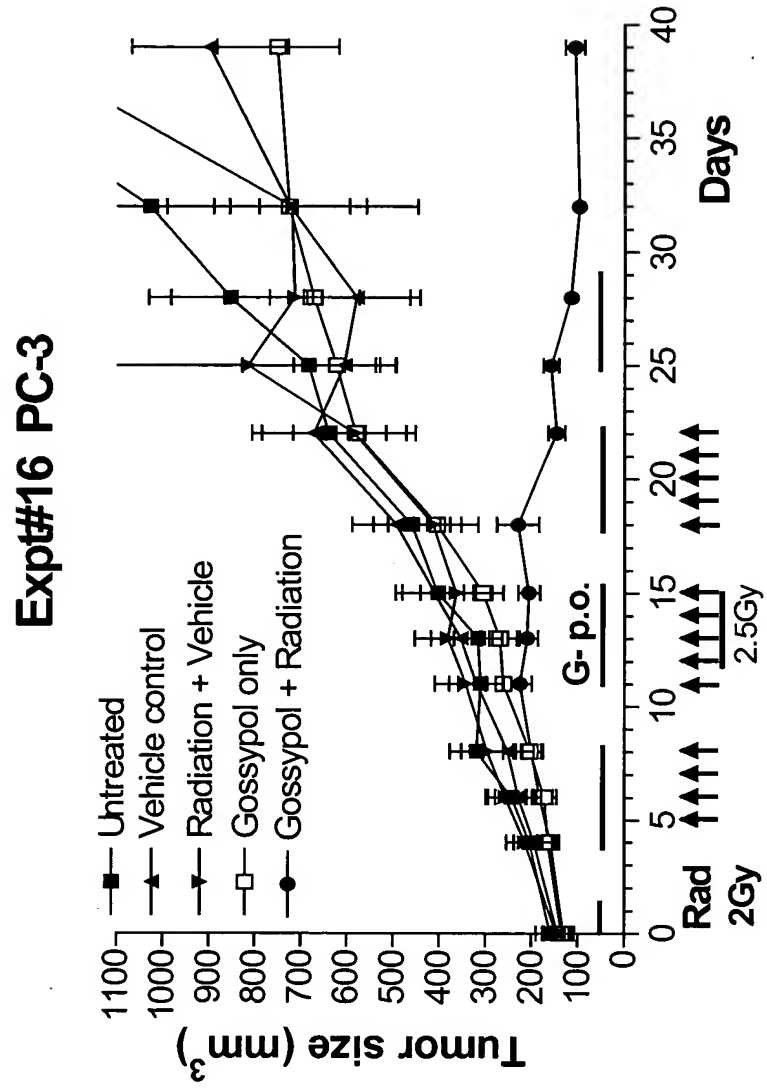


Figure 37

(-)-gossypol in combination with radiation in an androgen-independent prostate PC-3 xenograft model

Expt#16 PC-3 Mice Body Weight

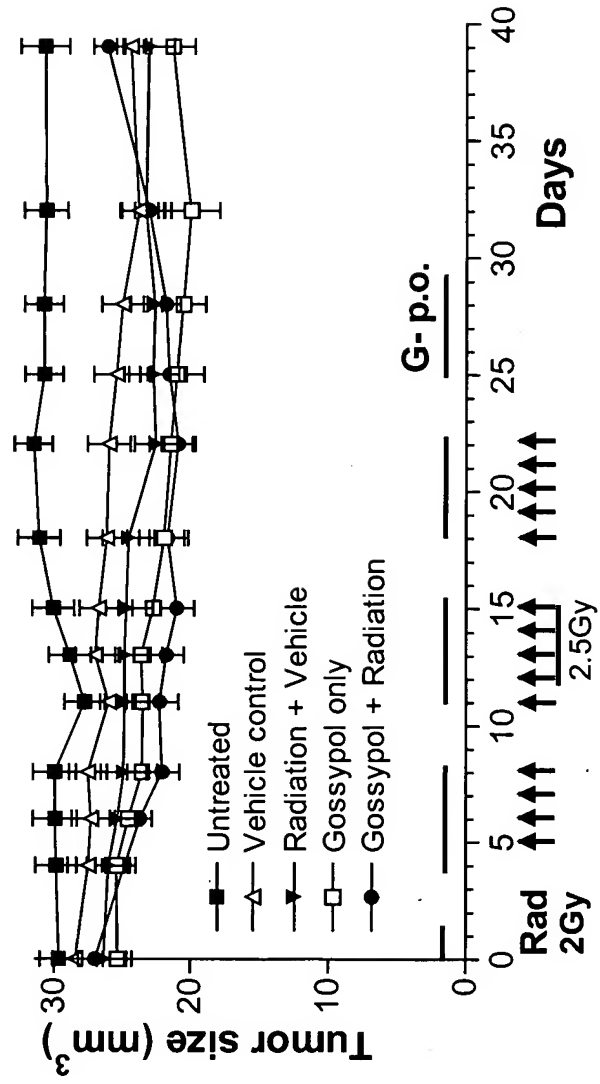


Figure 38

(-)-gossypol in combination with radiation in an androgen-independent prostate PC-3 xenograft model

PC-3

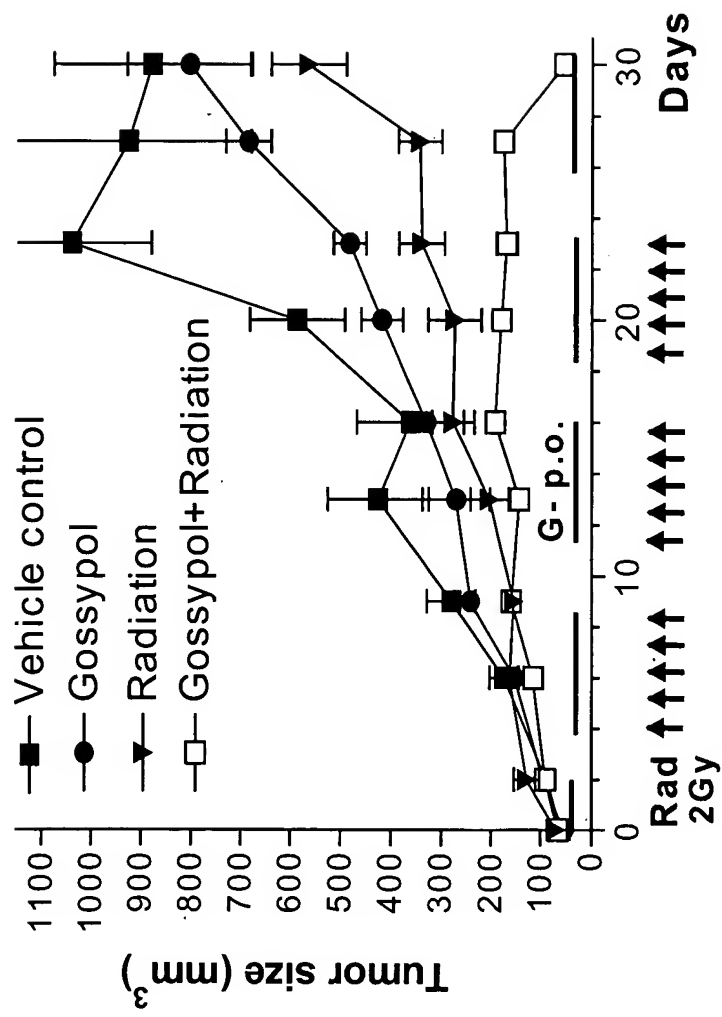
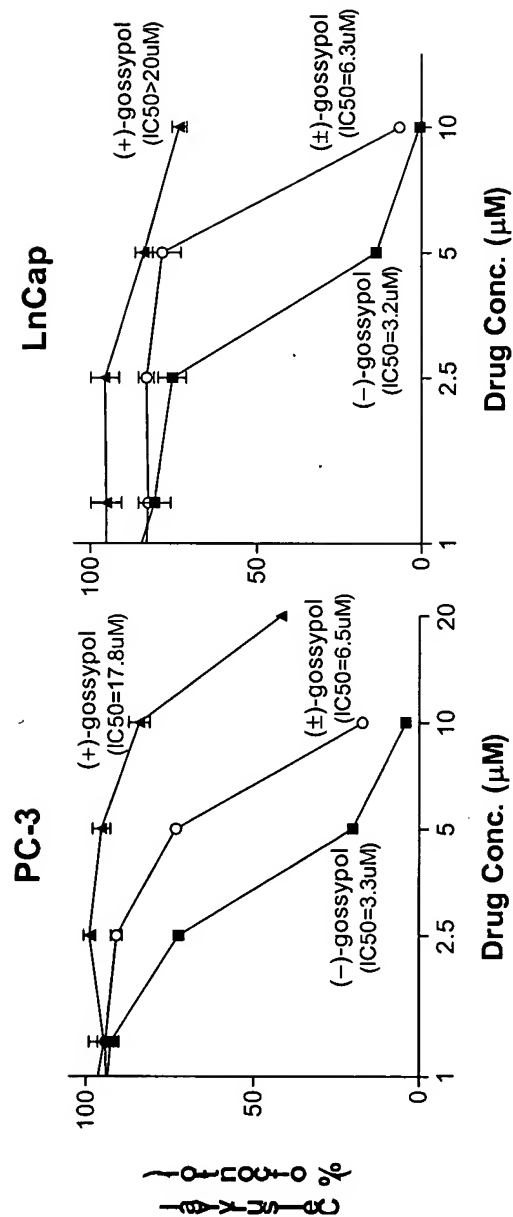
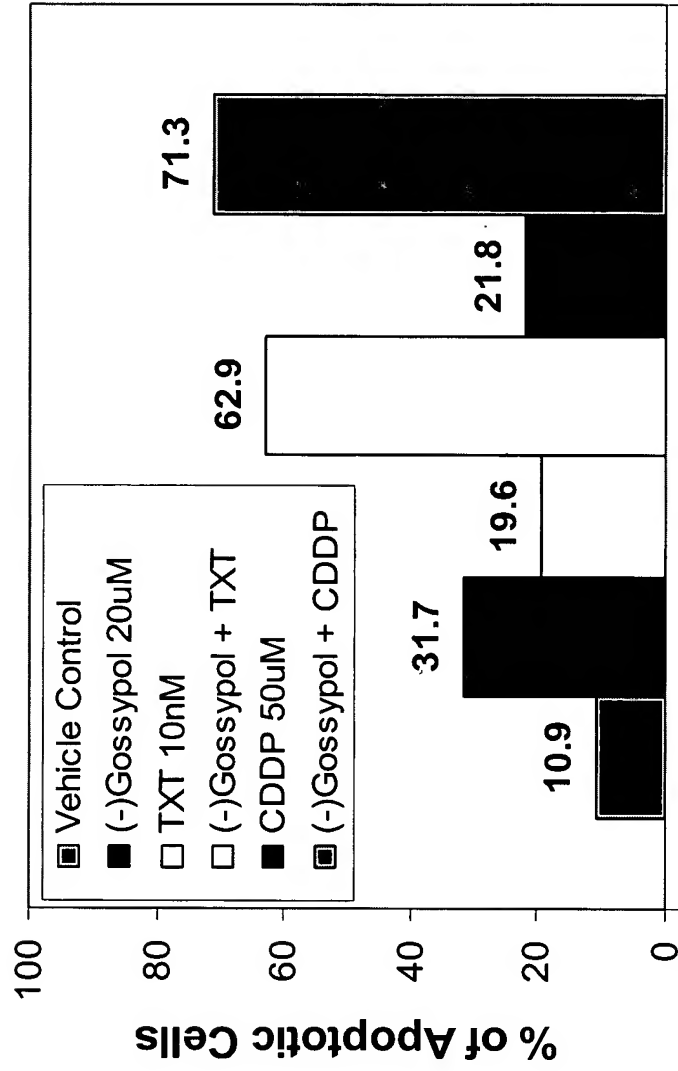


Figure 39



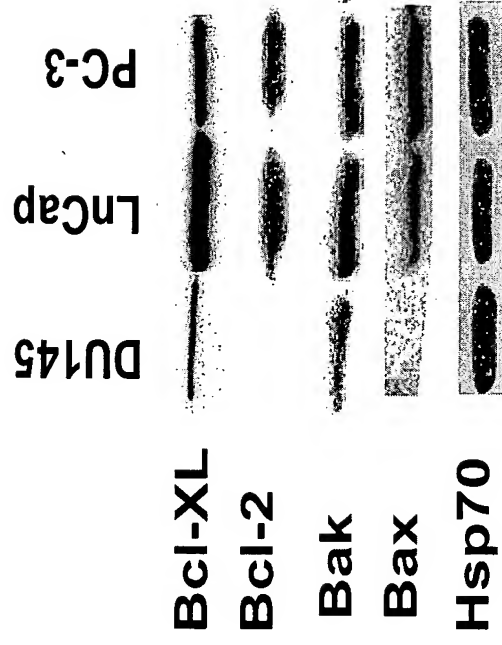
Prostate cancer cell growth inhibition by gossypol. PC-3 and LnCap cells in 96-well plates were treated in triplicates with gossypol and its enantiomers. MTT-based 5-day cell proliferation assay was performed and IC₅₀, drug concentration that inhibited 50% of cell growth, was calculated. (-)-gossypol is 5-10 times more potent than (±)-gossypol, 2 times more potent than (+)-gossypol, in both cell lines.

Figure 40



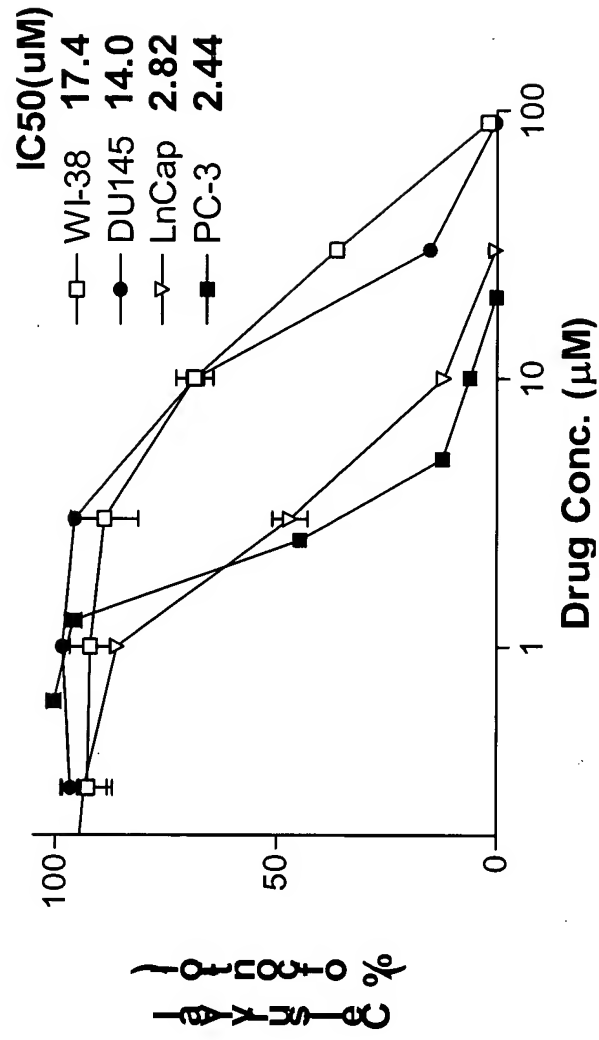
(-)Gossypol enhances chemotherapy-induced apoptosis in human prostate cancer PC-3 cells. Cells were treated with (-)gossypol alone or in combination with TXT or CDDP for 48hr, then stained with Annexin V-FITC and PI for flow cytometry. Values are % of apoptotic cells.

Figure 41



Basal levels of Bcl-2 family proteins expression in three prostate cancer cell lines. HSP70: heat shock protein 70kDa for gel loading control.

Figure 42



Cytotoxicity of (-)-gossypol on prostate cancer cells. MTT-based 5-day cell proliferation assay was performed and IC50, drug concentration that inhibited 50% of cell growth, was calculated.

Figure 43A

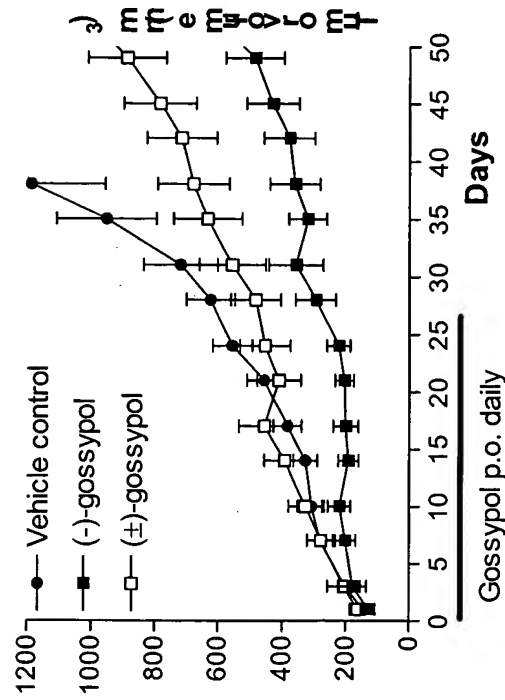
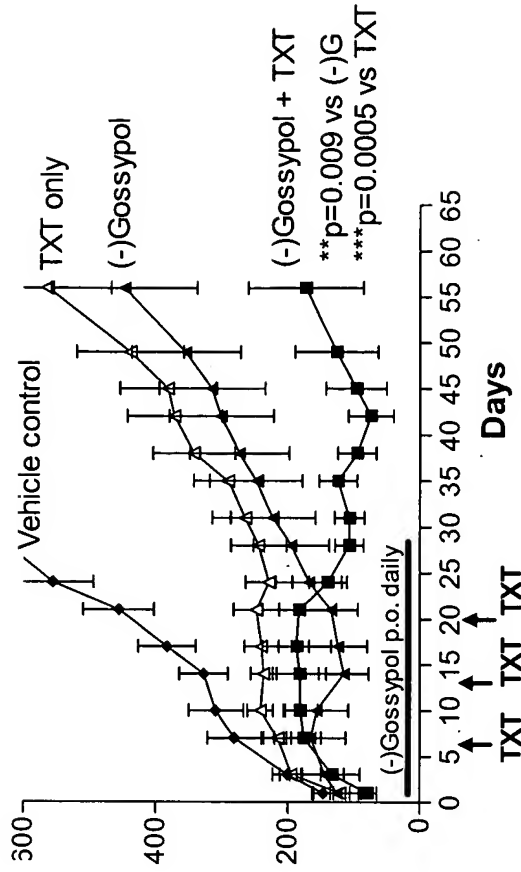


Figure 43B



In vivo anti-tumor activity of gossypol in human prostate cancer PC-3 xenograft model. A: 15mg/kg (±) or (-)-gossypol p.o. daily for 26 days. (-)-gossypol is more potent than (±)-gossypol ($P<0.001$). B: Tumor growth inhibition by (-)-gossypol was significantly enhanced when used in combination with docetaxel (TXT). **Student's t-test.

Figure 44

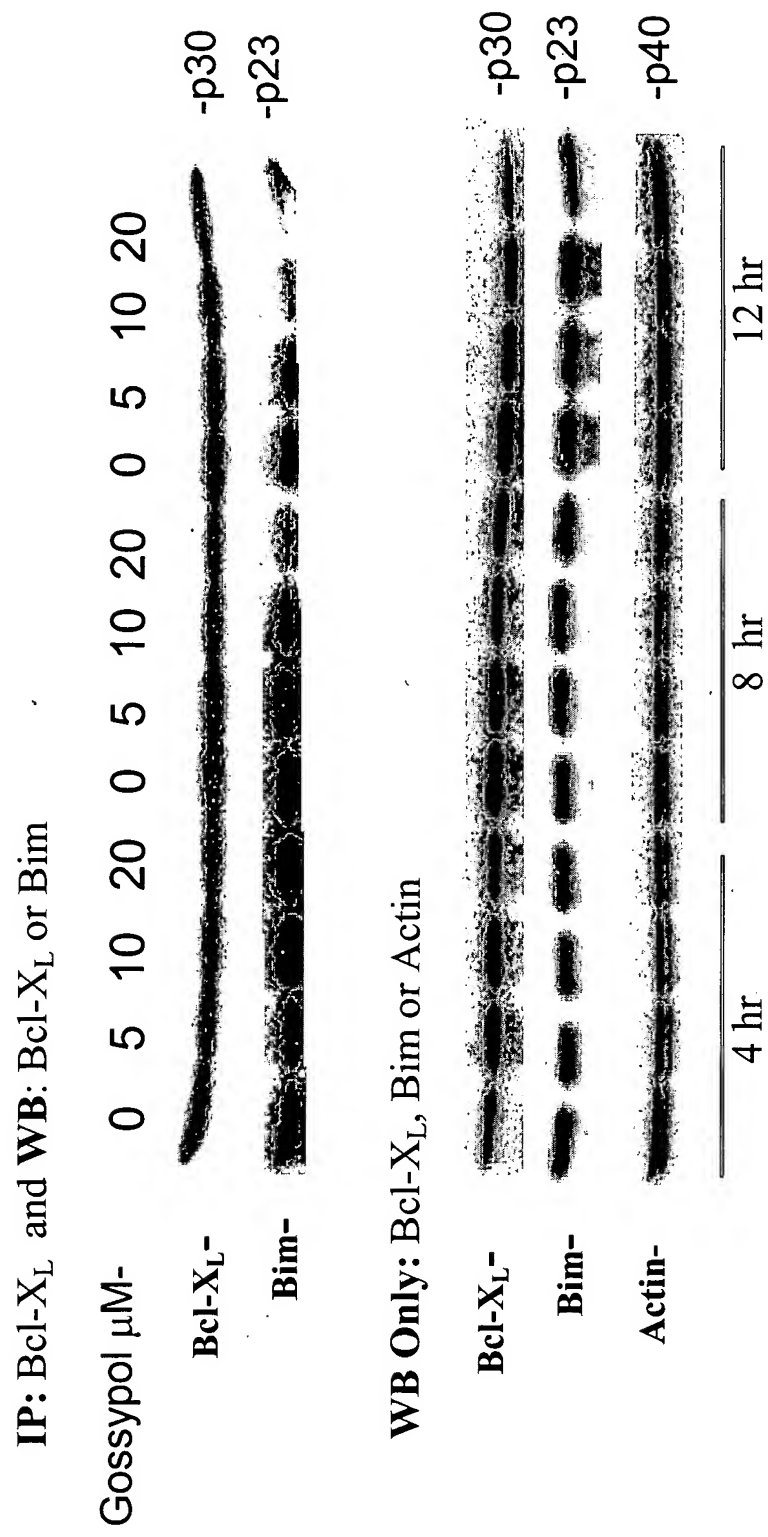


Figure 45

Competitive binding curve of apogossypol against Bcl-2

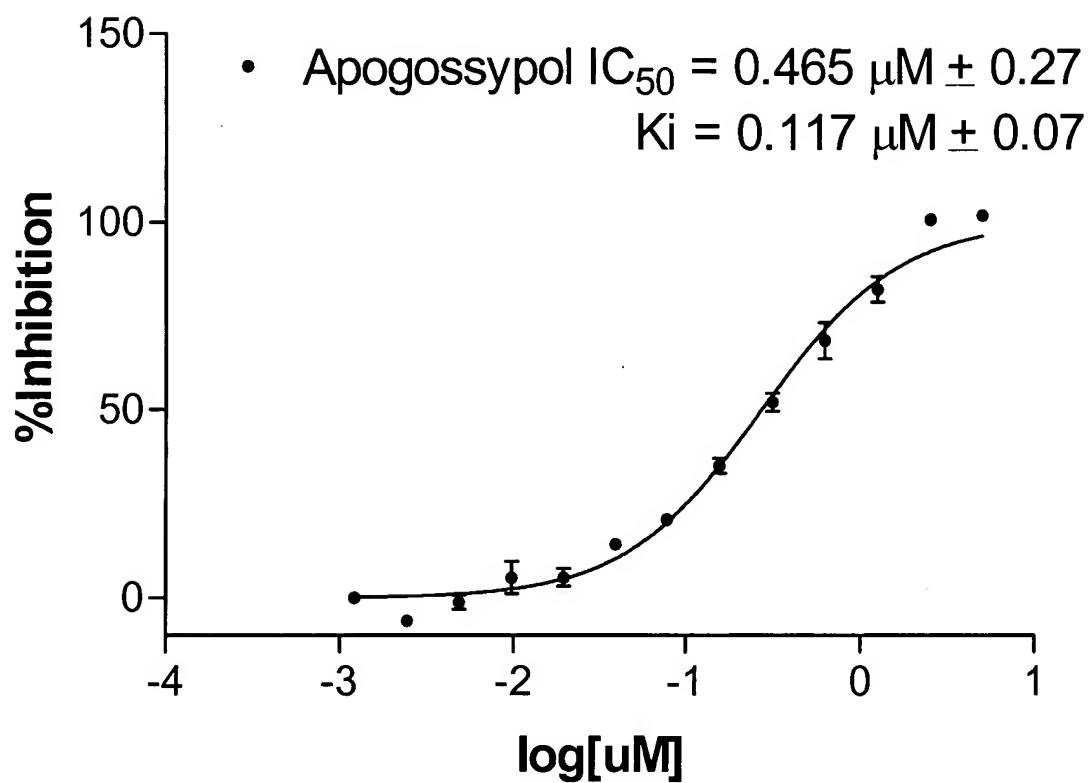


Figure 46

Competitive binding curve of apogossypol against Bcl-X_L.

